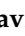




Article

Estimating Adaptive Setpoint Temperatures Using Weather Stations

David Bienvenido-Huertas ¹, Carlos Rubio-Bellido ^{2,*}, Juan Luis Pérez-Ordóñez ³
and Fernando Martínez-Abella ³

¹ Department of Graphical Expression and Building Engineering, University of Seville, 41012 Seville, Spain; jbienvenido@us.es

² Department of Building Construction II, University of Seville, 41012 Seville, Spain

³ Department of Civil Engineering, University of A Coruña, E.T.S.I. Caminos, Canales, Puertos Campus Elviña s/n, 15071 La Coruña, Spain; jlperez@udc.es (J.L.P.-O.); fmartinez@udc.es (F.M.-A.)

* Correspondence: carlosrubio@us.es; Tel.: +34-686-135-595

Received: 9 February 2019; Accepted: 23 March 2019; Published: 27 March 2019



Abstract: Reducing both the energy consumption and CO₂ emissions of buildings is nowadays one of the main objectives of society. The use of heating and cooling equipment is among the main causes of energy consumption. Therefore, reducing their consumption guarantees such a goal. In this context, the use of adaptive setpoint temperatures allows such energy consumption to be significantly decreased. However, having reliable data from an external temperature probe is not always possible due to various factors. This research studies the estimation of such temperatures without using external temperature probes. For this purpose, a methodology which consists of collecting data from 10 weather stations of Galicia is carried out, and prediction models (multivariable linear regression (MLR) and multilayer perceptron (MLP)) are applied based on two approaches: (1) using both the setpoint temperature and the mean daily external temperature from the previous day; and (2) using the mean daily external temperature from the previous 7 days. Both prediction models provide adequate performances for approach 1, obtaining accurate results between 1 month (MLR) and 5 months (MLP). However, for approach 2, only the MLP obtained accurate results from the 6th month. This research ensures the continuity of using adaptive setpoint temperatures even in case of possible measurement errors or failures of the external temperature probes.

Keywords: adaptive setpoint temperature; weather station; multivariable linear regression; multilayer perceptron

1. Introduction

1.1. Energy Consumption of Residential Buildings

Global warming, resource depletion, extinction of species, and melting of glaciers constitute the main concerns faced by current society [1]. One of the main causes of such situations is the greenhouse gases emitted to the atmosphere due to the energy consumption from the most important industries and sectors. In this way, building sector is among those most contributing to this situation. Approximately, buildings are responsible for between 30% and 40% of the total energy consumption [2], emitting 40% of the total greenhouse gas emissions [3,4]. Also, social and health aspects, such as energy poverty [5] or the increase of the death rate because of high temperatures [6,7], also constitute worrying aspects to be solved. Consequently, institutions promote more and more the improvement of efficient energy of the existing buildings. The European Union has established goals to reduce the energy consumption and CO₂ emissions by 2020, although such goals are proving difficult to

achieve because both the measures adopted and the proximity of the deadline are not quite effective. Under this circumstance, the European Union has set a greater goal by 2050, with the aim of having a low-carbon economy [8].

The improvement of the energy performance has been traditionally focused on improving the envelope by reducing the thermal transmittance of its elements. However, the improvement of the performance and the use of HVAC systems have been scarcely studied, despite their high effect on the energy consumption of a building [9]. Likewise, the large number of buildings with HVAC systems is relevant to establish energy conservation measures. In Spain [10], more than 50% of buildings have envelopes with values of thermal transmittance meeting the state regulations [11]. Thus, the improvement of active systems in buildings with not enough effective systems or the improvement of their use can constitute possible energy conservation measures. In this research, given the influence of users on energy consumption [12], the decrease of such consumption is suggested by providing more adequate guidelines of using such systems, that is, by modifying the setpoint temperatures [13].

1.2. Adaptive Setpoint Temperatures

The influence of setpoint temperatures on the energy consumption has been analysed in many research studies: (i) Sánchez-García et al. [14] studied the use of a configuration of thermal comfort, which was different from that used by the regulation in Spain, as an energy conservation measure in office buildings. The results allowed the heating and cooling energy consumption to be reduced between 50% and 61%; (ii) in a later study, Sánchez-García et al. [13] analysed the potential of using mixed modes with adaptive setpoint temperatures in office buildings. The results allowed both the energy demand and energy consumption to be reduced by 74.6% and 59.7%, respectively, with respect to the reference model; (iii) Sánchez-Guevara Sánchez et al. [15] applied monthly variations of setpoint temperatures to a social housing, reducing the energy requirement between 20% and 80%; (iv) Spyropoulos and Balaras [16] evaluated the possibility of reducing the energy consumption in 39 bank branches in Greece by modifying the setpoint temperatures. A temperature of 26 °C for the upper limit and 20 °C for the lower limit resulted in a saving of 45% in the energy consumption; (v) Yun et al. [17] studied the improvement of using an adaptive comfort model in setpoint temperatures of office buildings. The energy consumption was decreased by 22%, and 87% of users had acceptable thermal comfort conditions; and (vi) Hoyt et al. [18] conducted a similar study in office buildings. The use of a setpoint temperature of 27.87 °C for cooling and 18.3 °C for heating reduced the energy consumption between 32% and 73%, according to the climate zone.

Residential buildings are characterized by combining the use of HVAC systems with natural ventilation (particularly in buildings located in warm regions). Natural ventilation is used when the external temperature values are acceptable. The HVAC system is used when external conditions exceed the limits of acceptability. Therefore, an energy saving can be achieved by using models of adaptive thermal comfort [14]. Such models are based on the natural tendency of people to adapt their clothing, metabolic rate, and psychological conditions to external climate variations under conditions of natural ventilation [19], thereby implying thermal comfort limits to be wider than those of the static models traditionally used [20].

One of the most developed models of adaptive thermal comfort is that included in EN 15251 [21]. This model can be used in those rooms occupied by users with a clothing level between 0.5 and 1 clo (1 clo = 0.155 (m²K)/W) and with a metabolic activity between 1 and 1.3 (1 met = 58 W/m²). The possibility of implementing such model is by modifying the setpoint temperatures of HVAC systems [14]. To do this, setpoint temperatures are adapted to the limits of the internal operative temperature (upper and lower) considered by EN 15251. This new setpoint temperature is known as adaptive setpoint temperature [14]. When the internal operative temperature is within the limits of EN 15251, active systems are not used, thus reducing the energy consumption. The use of such setpoint temperatures allows significant decreases to be obtained depending on the case study and the

climate zone [14,15,22]. The results show a decrease between 10% and 18% in the cooling consumption by using adaptive comfort models. To determine the limit values of EN 15251, the equations used are as follows:

$$T_{rm} = 0.2 \cdot \sum_{i=1}^n (0.8^{i-1} \cdot T_{ext,i}) \quad (1)$$

$$T_{i,max} = 0.33 \cdot T_{rm} + 18.8 + \gamma \quad (2)$$

$$T_{i,min} = 0.33 \cdot T_{rm} + 18.8 - \gamma \quad (3)$$

where T_{rm} is the running mean temperature ($^{\circ}\text{C}$), $T_{ext,i}$ is the external temperature from the previous day i of the day when the running mean temperature ($^{\circ}\text{C}$) is calculated, $T_{i,max}$ is the upper limit value of the internal operative temperature ($^{\circ}\text{C}$), $T_{i,min}$ is the lower limit value of the internal operative temperature ($^{\circ}\text{C}$), and γ is the value of the level of expectation ($^{\circ}\text{C}$). The value of the acceptability level is determined according to the category of intervention distinguished by EN 15251 (see Table 1).

Table 1. Categories of EN 15251 and acceptability levels.

Categories	Description	γ
I	High level of expectation. The standard recommends its use in buildings occupied by weak and sensitive people, with special requirements (e.g., sick people, children or elderly).	2
II	Normal level of expectation. The standard recommends its use in new and renovated buildings.	3
III	Moderate level of expectation. The standard recommends its use in existing buildings.	4

It is worth noting that adaptive setpoint temperatures are determined by using external temperature values. For their application to real cases, external temperature probes are required [14].

However, measuring the external temperature correctly can be a challenge. As it is known, any sensor installed in the exterior is at the mercy of being influenced by the external weather. The main causes for measurement errors in external temperature probes are the solar radiation and the wind [23]. The effect of the solar radiation is quite significant in probes because of the warming generated in the sensor [24–26]. Therefore, the error generated in the sensor increases as the solar radiation is higher [27]. Thus, the sensors installed in façades with a high solar radiation (e.g., façades facing east or west) can present distortions in measurements. Also, reflected radiation sources, such as the albedo of surfaces covered by snow [28,29] and the zenith angle of the sun [30,31], can also distort temperature measurements. Such measurement errors can be of several degrees [29,32,33].

The lack of radiant elements does not mean the lack of distortions in measurements. Even when there are robust instruments and no radiant elements affecting the probe, the measurement of the air temperature can be influenced by the wind action over the surface of the sensor, the existing vegetation, and close buildings [31,34]. Likewise, performing accurate measurements of the external air temperature is something of a challenge when there is a thermal gradient in a short distance, such as the existing area under the awning [35].

Thus, the implementation of adaptive setpoint temperatures in buildings can be limited if the external temperature probes are not installed under adequate conditions, or even if the probe gets damaged due to the lack of a good maintenance plan. This could result in a mistaken estimation of the adaptive setpoint temperatures. For this reason, new methodologies to determine the adaptive setpoint temperatures are suggested in this research. Data from weather stations of official meteorological agencies were used, thereby guaranteeing that data from installations do not present errors because of environmental aspects as well as that equipment is correctly installed thanks to the maintenance plans of such agencies. Also, adaptive setpoint temperatures are used without having external probes, thus ensuring both the economic saving in the investment and a greater implementation rate. To determine the adaptive setpoint temperatures, two different approaches were used, and two different regression algorithms (multivariable linear regression and multilayer perceptron) were in turn used in each approach.

This article is divided as follows: Section 2 describes the methodology, that is, characteristics of the equipment used, the approaches to determine the adaptive setpoint temperatures, the regression algorithms, and the procedures of training and validation of models. Section 3 discusses the results obtained. Finally, Section 4 summarizes the main conclusions.

2. Methodology

2.1. Case Study

Galicia is the autonomous community located in the northwest region of Spain (Figure 1). This region covers an area of 29,575 km², with a population of 2,701,743 people in 2018 [36,37]. In this area, the climate is oceanic Mediterranean (Csb) according to the Köppen-Geiger climate classification [38]. This climate typology is found in various other geographical points of the planet, such as Chile or the United States [38]. However, the climate in Galicia is influenced by the topography of the region. The topography significantly influences climate because precipitation pattern, relative humidity, temperatures, and solar radiation will vary according to the altitude [39–42]. Thus, in Galicia, where the altitude varies from 0 to more than 1000 m above sea level, there are various microclimates [43]. In this way, the Spanish Building Technical Code distinguishes six different climate zones according to the climate severity of winter and summer [11].

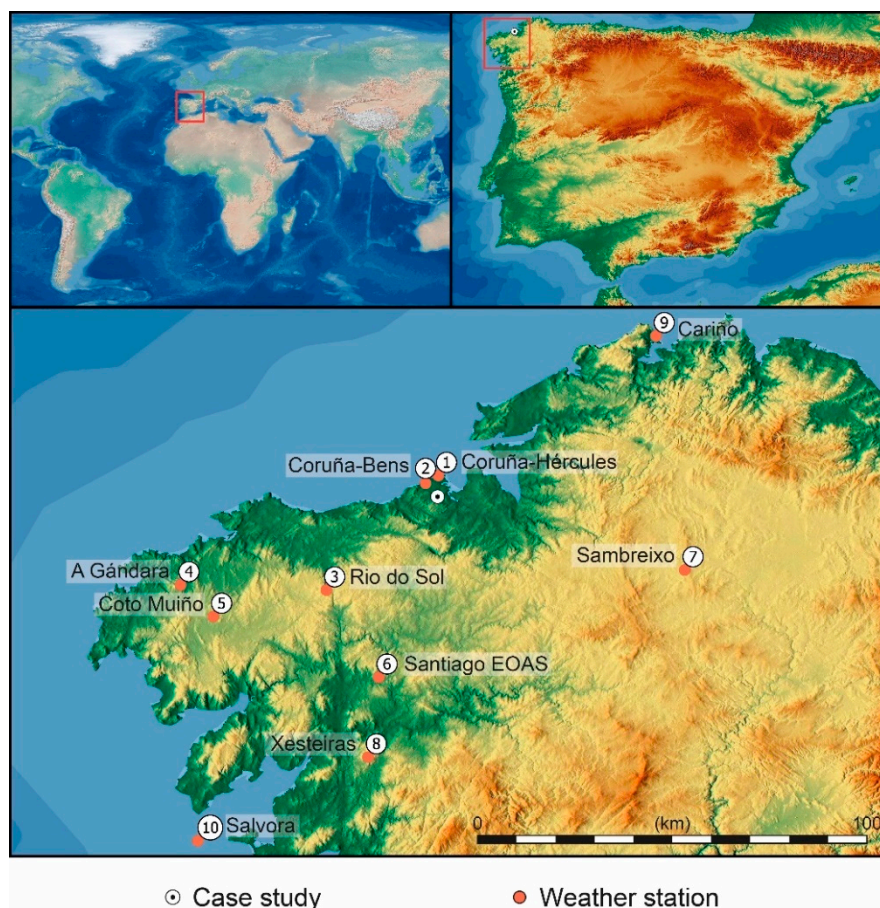


Figure 1. Location of the case study and the weather stations used. Further information of the weather stations can be found in Table 3.

The case study is located in San Vicente de Elviña (Figure 1), at a latitude of 43.33001 and a longitude of -8.41179 (WGS84 coordinate system). It is at an altitude of 55 m. The temperature and the relative humidity were monitored using a CR1000 datalogger (Campbell Scientific, Logan,

UT, USA) with a HC2S3 sensor (Figure 2). The technical specifications of the probe are indicated in Table 2. The measurement interval was 30 min throughout almost 3 years (from 12 February 2016 to 17 December 2018). Each instance of the dataset was the average of 1800 measures. The sensor was placed in a pole closed to the wall of the case study, at a distance of 20 cm from the façade and 150 cm from the slab. The sensor was located facing north to avoid the effects of solar radiation [44]. Also, the sensor had a Campbell RAD10 multi-plate radiation shield. By obtaining the measurements of the external temperature, the adaptive setpoint temperatures (upper and lower limits) could be determined for categories I, II, and III from EN 15251.



Figure 2. Temperature probe of the case study.

Table 2. Technical specifications of the external temperature probe used.

Technical Specification	Values
Measurement Range	−50 to 100 °C (default −40 to 60 °C)
Output Signal Range	0 to 1 V
Accuracy	±0.1 °C with standard configuration settings (at 23 °C)
Long-Term Stability	<0.1 °C/year

2.2. Weather Stations

As mentioned in Section 1, the objective of this research was determining adaptive setpoint temperatures without using external temperature probes. For this purpose, data from weather stations of an official meteorological agency, MeteoGalicia, were used. MeteoGalicia is a meteorological agency which is dependent of the Consellería de Medio Ambiente, Territorio e Infraestruturas of the Xunta de Galicia. Nowadays, such agency includes in its website a wide variety of environmental observation datasets from different weather stations.

The weather stations selected for this study were as follows: Coruña-Hércules, Coruña-Bens, Rio do Sol, A Gándara, Coto Muiño, Santiago EOAS, Sambreixo, Xesteiras, Cariño, and Salvora. From such stations, the values of the average daily temperature at 1.5 m, which were registered in the same test period that the case study, were compiled. As can be seen in Figure 1 and Table 3, such weather stations were selected because they present important differences in the altitude and the distance between coordinates with respect to the case study. The average values of the daily external temperature had therefore differences with respect to the case study (Figure 3). In this sense, the weather stations located in areas with a high altitude, such as Sambreixo or Xesteiras, presented different temperature distributions. With this aspect, the limitations that may exist in the methodologies used in case of using data from weather stations under different climate conditions were assessed.

Table 3. Coordinates of the weather stations.

Weather Station	Latitude ^a	Longitude ^a	Altitude (m)	Distance from the Case Study (m)	Height Difference with Respect to the Case Study (m)
1. Coruña-Hercules	43.3829	−8.40993	21	5883.02	−34
2. Coruña-Bens	43.3634	−8.44187	131	4438.60	76
3. Rio do Sol	43.0952	−8.69099	540	34,549.61	485
4. A Gándara	43.1081	−9.05694	405	57,808.57	350
5. Coto Muiño	43.028873	−8.974914	317	56,622.68	262
6. Santiago EOAS	42,876	−8.55944	255	51,887.22	200
7. Sambreixo	43.1457	−7.79112	496	54,295.09	441
8. Xesteiras	42.6756	−8.58618	715	74,136.00	660
9. Cariño	43,734	−7.86335	5	63,029.12	−50
10. Salvora	42.4649	−9.01364	24	107,967.54	−31

^a WGS84 coordinate system.

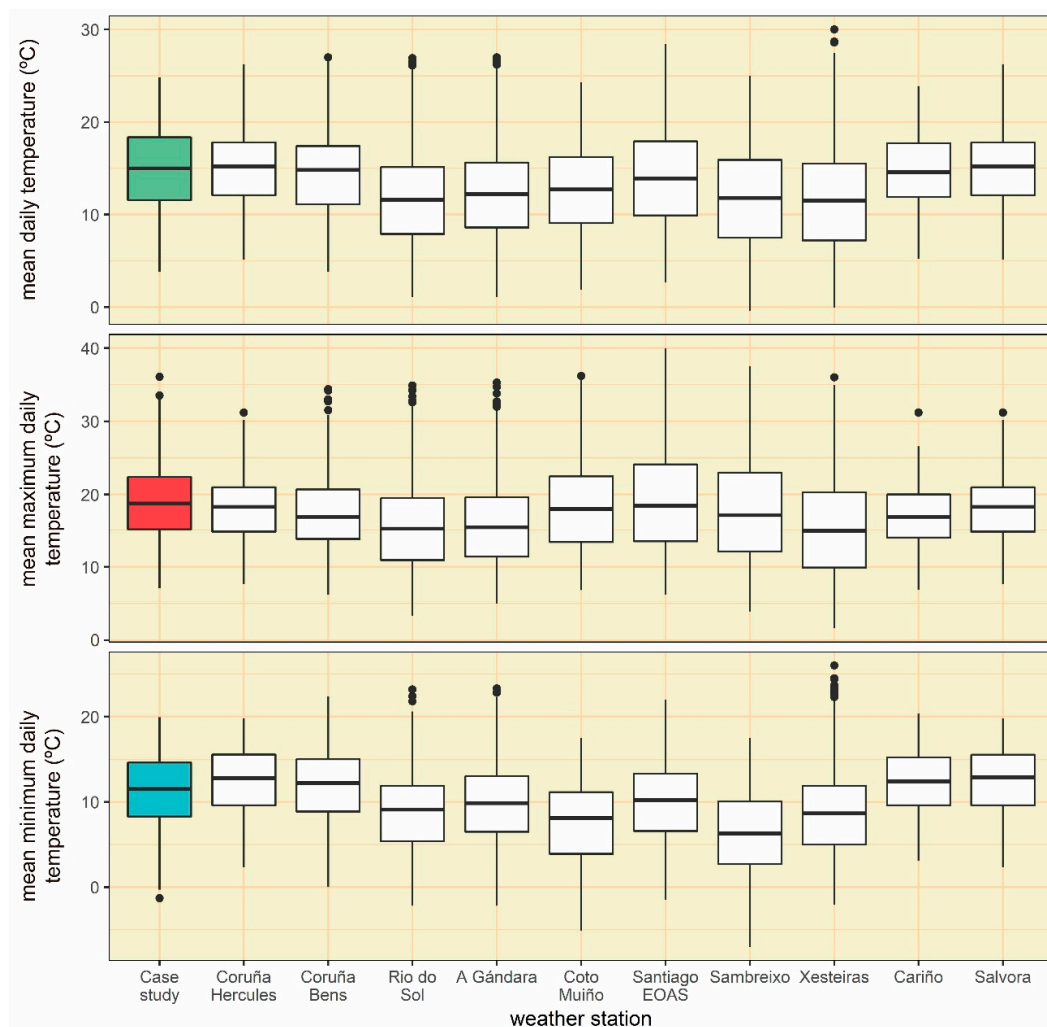


Figure 3. Box-plots of the daily temperatures of the case study and the weather stations. The upper and bottom lines represent 25% of the data distribution of maximum and minimum values, respectively. The points are outliers in the data distribution.

The temperature values obtained by the weather stations were measured by using the sensors indicated in Table 4. Despite sensors are designed for being used under unfavourable external conditions (e.g., rainfalls or solar radiation), they were installed inside a protection box to guarantee that the data registered by the sensors of each weather stations did not present errors.

Table 4. Temperature and humidity sensors of each weather station.

Sensor	Measurement Range	Accuracy	Weather Station
Vaisala HMP155	−80–60 °C	±0.25 °C	Coruña-Hércules, Coruña-Bens, Río do Sol, A Gándara, Coto Muiño, Sambreixo, Cariño, Salvora
Geónica STH-5031	−40–60 °C	±0.10 °C	Santiago EOAS
Rotronic HC2A-S3	−50–100 °C	±0.30 °C	Xesteiras

2.3. Approaches for Estimating Adaptive Setpoint Temperatures

To estimate the adaptive setpoint temperatures, two approaches were designed (Table 5): (i) approach 1, where the adaptive setpoint temperature is determined with the adaptive setpoint temperature from the previous day and the mean daily external temperature from the previous day of the weather station; and (ii) approach 2, where the adaptive setpoint temperature is determined with the mean daily temperatures of the 7 previous days. Such approaches were designed in accordance with criteria from EN 15251 to estimate the limits of adaptive thermal comfort. Moreover, they were designed to estimate both upper and lower limits. Input and output variables were used by the regression algorithms described in Section 2.4 to generate prediction models of each weather station.

Table 5. Input and output variables for each approach.

Approach	Input Variables	Output Variables
Approach 1	$T_{ext,d-1}, T_{sp,d-1}$ ^a	$T_{sp,d}$ ^a
Approach 2	$T_{ext,d-1}, T_{ext,d-2}, T_{ext,d-3}, T_{ext,d-4}, T_{ext,d-5}, T_{ext,d-6}, T_{ext,d-7}$	$T_{sp,d}$ ^a

$T_{ext,d-n}$: mean daily external temperature from the previous n days; $T_{sp,d-1}$: adaptive setpoint temperature from the previous day; $T_{sp,d}$: adaptive setpoint temperature from the current day. ^a Adaptive setpoint temperature corresponding to the upper and lower limit. Regarding approach 1, the limit of the adaptive setpoint temperature will be the same for both input and output variable.

2.4. The Regression Algorithms Used

To generate the prediction models, two regression algorithms were used: a multivariable linear regression (MLR) and a multilayer perceptron (MLP).

2.4.1. MLR

MLR is a classic regression algorithm which connects a dependent variable (y_i) with independent variables p :

$$y_i = \beta_0 + \sum \beta_p X_{pi} + \varepsilon_i \quad (4)$$

where X_{pi} are the independent variables (also called explicative), p is the number of the independent variables, β_0 is the constant term, β_p is the influence of variables on the dependent variable, and ε_i is the term of error (also called term of noise).

MLR is based on a linear statistical model without needing adjustment parameters, and this is an advantage by applying it [45]. Another advantage is understanding the existing relationship between the independent variables and the dependent variable [46]. Such algorithm has therefore been widely used to estimate and predict in the energy analysis of buildings: (i) Pulido-Arcas et al. [46] developed 18 MLRs to estimate the energy consumption and CO₂ emissions in office buildings which were located in 9 cities of Chile. The correlation coefficient obtained by the models ranged between 91.81% and 99.56%, thereby reflecting the possibilities of using such models for the energy characterization of office buildings; (ii) Qiang et al. [47] developed MLR models to estimate the daily mean cooling load in HVAC systems of office buildings in Tianjin (China). The estimations obtained by the models presented a mean absolute percentage error lower than 8% with respect to the real values; (iii) Amber et al. [48] developed an MLR to estimate the daily energy consumption in university buildings. The independent variables of the model were external temperature, relative humidity, solar

radiation, wind speed, weekday index (1 for working days and 0 for the remaining days), and type of building. The results obtained error parameters between 12% and 13% according to the type of building analysed; (iv) a wider approach was given by Kialashaki and Reisel [49]. These authors developed MLRs to estimate the energy demand of the residential building stock in United States. The performance of the models obtained correlation coefficients greater than 95%; and (v) the problem of reducing the energy consumption in the design phase was analysed by Asadi et al. [50]. In such study, the use of MLRs to estimate the energy consumption of commercial buildings was assessed by using the input variables of the envelope and the morphology of the building, as well as the building occupancy schedule.

2.4.2. MLP

MLPs simulate, through mathematical models, the behaviour of the nervous system. As in the biological model, the artificial neuron is in charge of receiving, processing, and transmitting information to the following multiple neurons [51]. The output information is obtained from the processing through the network of the input information (Figure 4). To integrate and compute the information from the environment and other neurons, the artificial neuron uses the propagation, activation, and transfer function. Generally, the propagation function (Equation (5)) is the sum of each input (p_j) multiplied by a weight (W_{ij}):

$$n_j = \sum_{i=0}^{n-1} W_{ji} p_i \quad (5)$$

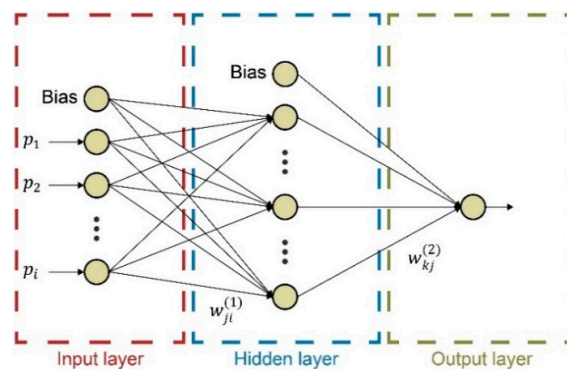


Figure 4. Example of an MLP of a hidden layer.

The activation function (AF) modifies the value obtained in the propagation function (Equation (6)), thus relating the input of each neuron to the next activation state. At the output of the neuron, there could be a threshold function establishing a limit value, which should be exceeded before being propagated to another neuron (Equation (7)). This function is known as the transfer function (TF). The next point to define an MLP is to determine the network topology to be used. MLPs are mainly divided into feedforward and feedback networks. The first network moves the information to a single direction (input towards output), and the second to any direction:

$$a_i(t) = AF(a_i(t-1), n_i(t-1)) \quad (6)$$

$$out_i = TF(a_i(t)) \quad (7)$$

where $n_j(t-1)$ is the input value of the neuron, a_j is the activation value, and t is the iteration.

MLPs constitute nowadays one of the most used regression algorithms because they generally have a better performance than other regression algorithms [52,53]. In consequence, they have been used in many research works to assess the energy performance of buildings and installations: (i) Attoue et al. [54] developed a model of artificial neural network to estimate the variation of the

internal temperature so that the energy consumption in the building could be optimized. By using the three-hour façade temperature history and the external temperature as input variables, the internal temperature could be suitably estimated until two hours after obtaining the input data; (ii) Zabada and Shahrour [55] carried out an analysis using an artificial neural network to assess the influence of different parameters on heating cases in social dwellings in France. Such analysis reflected that some parameters, such as the surface of the dwelling, date of construction, and the energy performance, influenced the heating consumption. Likewise, social indicators such as family size, member age, and tenant income influenced the heating expense; (iii) Yu et al. [56] developed an MLP to estimate the heating energy demand in residential buildings. The model was validated with actual demand values in residential buildings of Chongqing (China). The errors of the estimation obtained by the model were lower than $\pm 2.5\%$; (iv) a similar approach was carried out by Deb et al. [57] to estimate the diurnal cooling load in institutional buildings. The MLP developed allowed the cooling loads in the following 20 days to be accurately predicted; and (v) Moon et al. [58] developed an MLP for the thermal control in buildings with double skin envelopes by using the air gap temperature and the internal and external air temperatures, among others, as input variables. The performance of the MLP was analysed for several opening strategies in heating or cooling situations.

2.5. Dataset, Training, and Testing of the Models

The development, validation, and testing of the approaches and the prediction models followed the flowchart of Figure 5. Firstly, measurements performed by the external probe of the case study and the weather stations of MeteoGalicía were compiled. Then, adaptive setpoint temperatures of the 3 categories from EN 15251 (Equations (1)–(3)) were determined. The running mean temperature was obtained through data of the temperature probe of the case study. It is worth highlighting that the limit value obtained from Equations (2) and (3) (e.g., for the upper limit of category III, temperatures of 26.10 and 32.70 were used for their minimum and maximum values, respectively) was used in those cases in that the running mean temperature is not within the application of the standard (i.e., when such temperature is not between 10 and 30 °C for the upper limit, and not between 15 and 30 °C for the lower limit).

The full dataset was generated by using such data, with a total of 1040 instances (measurement days). Both the training and testing dataset were generated with such dataset (Table 6). The training datasets were used to generate individual models for each weather station as well as for each limit of adaptive setpoint temperature (upper or lower), using MLR or MLP as regression algorithms. To generate the MLR models, the Akaike information criterion was used [59].

Table 6. Datasets used.

Dataset	Number of Instances (days)	First Date	Last Date
Training	365	12 February 2016	11 February 2017
Testing	675	12 February 2017	17 December 2018

For the MLPs, only architectures of three layers (input, hidden, and output layers) were used because they generally have performances better than more complex architectures [60]. The sigmoid function has been selected as a transfer function. In the training of the MLPs, the Broyden-Fletcher-Goldfarb-Shanno (BFGS) algorithm [61] has been chosen, thus minimizing the mean squared error of the difference between the outputs in each step. Likewise, the training was carried out using a 10-fold cross validation, thereby dividing randomly the training dataset into 10 subsets: for each fold, 9 subsets were used as a training dataset, and the remaining subset was used to assess the performance of each model. Through this procedure, both the error and the variance of the model decreased [62].

The testing dataset was used to determine the error of generalization of the models obtained in the training phase. The performance of each model was assessed by analysing three quality statistical

parameters: the linear correlation coefficient (R^2) (Equation (8)), the mean absolute error (MAE) (Equation (9)), and the root mean square error ($RMSE$) (Equation (10)):

$$R^2 = \left(1 - \frac{\sum_{i=1}^n (t_i - m_i)^2}{\sum_{i=1}^n (t_i - \bar{t}_i)^2} \right) \quad (8)$$

$$MAE = \frac{\sum_{i=1}^n |t_i - m_i|}{n} \quad (9)$$

$$RMSE = \left(\frac{\sum_{i=1}^n (t_i - m_i)^2}{n} \right)^{1/2} \quad (10)$$

where m_i is the model's estimation, t_i is the actual value of adaptive setpoint temperature, and n is the number of observations in the dataset.

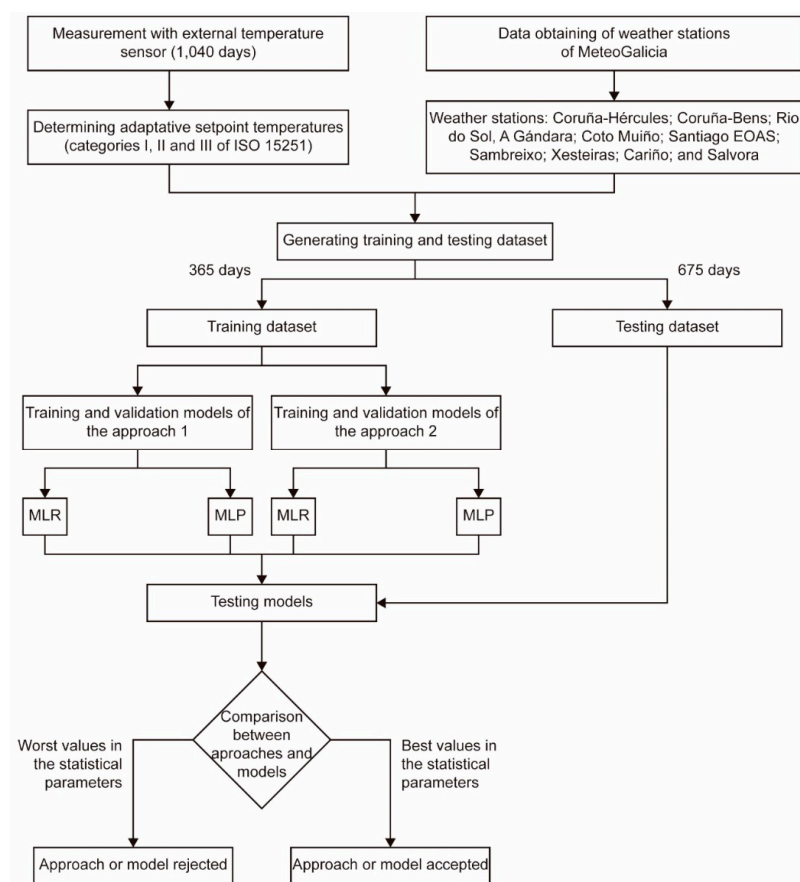


Figure 5. Flowchart of this research.

3. Results and Discussion

After generating the dataset, the estimation models were analysed. This section is structured by distinguishing the approach used and the performance obtained by the MLR and MLP models in each of them. As mentioned in Section 2.5, all models were created by using a training dataset of 1 year, and the testing dataset corresponds to the remaining period of time (675 days). Based on the similarity of the results of the statistical parameters of the models for the three categories of EN 15251, the values of category III are indicated in the following tables to make its reading easier because variations presented by the statistical parameters between the different categories were lower than 2%. Appendix A shows the point clouds between the actual and estimated values for the different categories so that the reader can visualize the accuracy level of the estimations performed by each model.

3.1. Approach 1: With the Setpoint Temperature and the External Temperature from the Previous Day

As mentioned above, this approach consisted of determining the adaptive setpoint temperature with external temperature data from the previous day ($T_{ext,d-1}$) and the adaptive setpoint temperature from the previous day ($T_{sp,d-1}$). Depending on the limit to be estimated (upper or limit), the setpoint temperature from the previous day for such limit is used.

It is worth noting the importance of using the setpoint temperature from the previous day. Such temperature was used because it generated an adjustment degree on the models. In this sense, Figures 6 and 7 show how including $T_{sp,d-1}$ generated a high adjustment between the actual and the estimated values. Despite the high adjustment obtained with $T_{sp,d-1}$, $T_{ext,d-1}$ is required to be considered as an independent variable because it reduces the error related to the estimations when the external temperature fluctuations are presented.

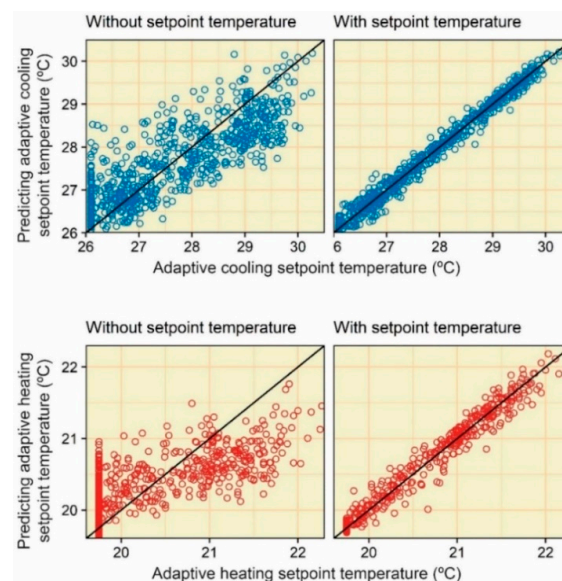


Figure 6. Influence of applying the setpoint temperature from the previous day on the MLR by using the external temperature of the weather station of Xesteiras.

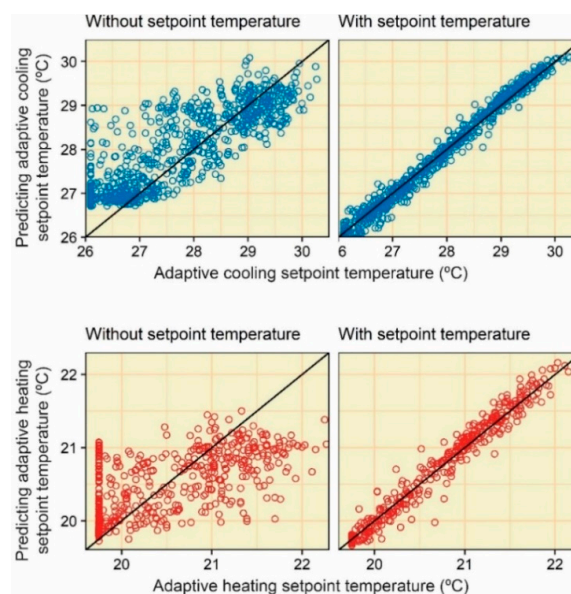


Figure 7. Influence of applying the setpoint temperature from the previous day on the MLP by using the external temperature of the weather station of Xesteiras.

3.1.1. MLR

First, the performance of approach 1 was analysed using the MLR as a regression algorithm. Table 7 indicates the performances obtained by the MLRs, and Figures A1–A3 and Figures A13–A15 in Appendix A show the point clouds between the actual and the estimated values of the different categories from EN 15251. As can be seen, the performance obtained by the MLRs was quite adjusted. In this sense, R^2 was always greater than 99% both in the training and the testing of the upper and lower limits. There were no great deviations in the estimation of the limit values (values which are not within the application of the standard), with a mean deviation value of 0.06 °C in these temperatures. Also, MAE and $RMSE$ were lower than 0.10 and 0.15, respectively, in the testing phase of almost all models, and only in some cases the error parameters were higher than these two values, although the increase in the error parameters was always lower than 25%. By using data from distant weather stations, a lower performance was not detected either. As seen in Section 2.2, the weather stations of Sambreixo, Xesteiras, Cariño, and Salvora were those more distant from the case study. The performances of the models generated with data from such weather stations were analysed, and the results obtained were similar to those from other nearer weather stations, even obtaining better performances (e.g., the MLPs of the weather station of Sambreixo, with statistical parameters better than those of the weather stations of Rio do Sol and A Gándara). Only the MLPs of the weather station of Xesteiras obtained a less adjusted performance than the other models, although the correlation coefficient was greater than 99%.

Table 7. Results of the training and testing of the MLR models of approach 1.

Model	Upper Limit			Lower Limit		
	R^2	MAE	$RMSE$	R^2	MAE	$RMSE$
Training						
Coruña-Hercules	99.71	0.0696	0.0911	99.01	0.0654	0.0936
Coruña-Bens	99.70	0.0694	0.0923	99.10	0.0650	0.0895
Rio do Sol	99.51	0.0887	0.1183	99.04	0.0640	0.0921
A Gándara	99.54	0.0876	0.1147	99.06	0.0642	0.0915
Coto Muiño	99.72	0.0689	0.0903	99.07	0.0649	0.0908
Santiago EOAS	99.72	0.0675	0.0901	99.07	0.0641	0.0911
Sambreixo	99.66	0.0774	0.0984	99.05	0.0651	0.0919
Xesteiras	99.36	0.1006	0.1356	99.00	0.0642	0.0940
Cariño	99.58	0.0815	0.1099	98.96	0.0643	0.0959
Salvora	99.71	0.0696	0.0911	99.01	0.0654	0.0936
Testing						
Coruña-Hercules	99.61	0.0774	0.1087	99.18	0.0679	0.0956
Coruña-Bens	99.52	0.1249	0.1525	99.22	0.0695	0.0954
Rio do Sol	99.53	0.0906	0.1218	99.21	0.0674	0.0937
A Gándara	99.54	0.0927	0.1209	99.21	0.0671	0.0941
Coto Muiño	99.76	0.0654	0.0853	99.27	0.0659	0.0905
Santiago EOAS	99.76	0.0649	0.0849	99.25	0.0667	0.0915
Sambreixo	99.61	0.0796	0.1077	99.17	0.0695	0.0964
Xesteiras	99.46	0.0999	0.1291	99.20	0.0671	0.0948
Cariño	99.62	0.0830	0.1076	99.11	0.0709	0.0999
Salvora	99.61	0.0774	0.1087	99.18	0.0679	0.0956

Another aspect to be considered was the minimum size of the training dataset to obtain valid results in the next months. Figure 8 shows how estimations with R^2 greater than 95% and values of MAE and $RMSE$ lower than 0.11 and 0.19, respectively, were obtained by using training sample of only a month. Moreover, the performance obtained was almost the same compared with the model generated with a training dataset of 1 year. The only requirement to obtain an accurate estimation is that the training period of 1 month is not composed only by days which are not within the limits of application (i.e., when the running mean temperature is not between 15 and 30 °C for the upper limit, and not between 10 and 30 °C for the lower limit). This aspect is quite relevant because, if the HVAC

system has an external temperature probe to record external temperatures, the predictive model could be generated by using data of a month, so the continuity of using adaptive setpoint temperatures is ensured even if the probe fails in a short period of time.

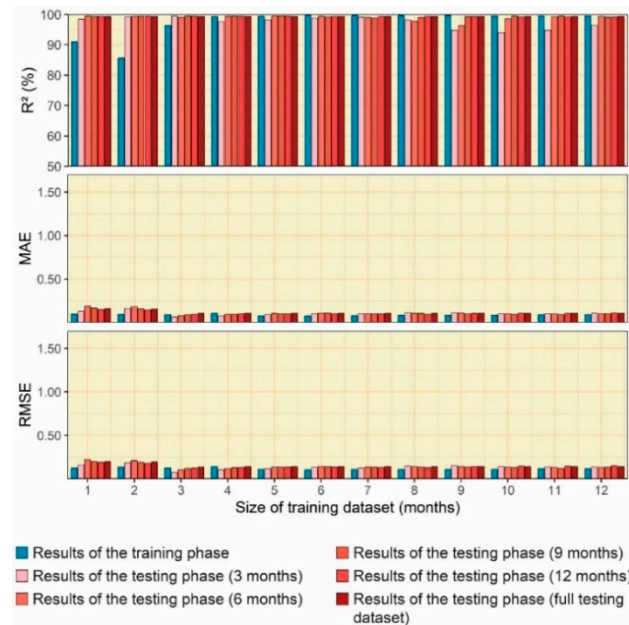


Figure 8. Influence of the size of the training sample on the MLR model (approach 1).

3.1.2. MLP

Despite the high performance obtained by the MLRs in approach 1, the MLPs were also analysed. Table 8 indicates the values of statistical parameters obtained in the training and testing phases of the different models.

Table 8. Results of the training and testing of the MLP models of approach 1.

Model	Upper Limit			Lower Limit		
	R^2	MAE	RMSE	R^2	MAE	RMSE
Training						
Coruña-Hercules	99.26	0.1112	0.146	98.99	0.0629	0.0969
Coruña-Bens	99.25	0.1117	0.1463	99.00	0.0623	0.0956
Río do Sol	99.24	0.1100	0.1480	99.01	0.0596	0.0940
A Gándara	99.19	0.1144	0.1521	98.98	0.0619	0.0956
Coto Muiño	99.28	0.1089	0.1437	99.03	0.0591	0.0932
Santiago EOAS	99.31	0.1073	0.1410	99.12	0.0595	0.0899
Sambreixo	99.34	0.1051	0.1380	99.06	0.0606	0.0917
Xesteiras	99.13	0.1168	0.1575	98.88	0.0627	0.0998
Cariño	99.21	0.1143	0.1505	98.92	0.0659	0.0980
Salvora	99.26	0.1112	0.1459	98.99	0.0640	0.0973
Testing						
Coruña-Hercules	99.31	0.1197	0.157	99.18	0.0743	0.1072
Coruña-Bens	99.39	0.1158	0.1499	99.07	0.1123	0.1604
Río do Sol	99.30	0.1313	0.1638	99.15	0.0790	0.1108
A Gándara	99.31	0.1284	0.1621	99.13	0.0743	0.1102
Coto Muiño	99.42	0.1260	0.1624	99.28	0.0830	0.1032
Santiago EOAS	99.46	0.1108	0.1438	99.34	0.0733	0.0961
Sambreixo	99.40	0.1414	0.1805	99.31	0.0808	0.1008
Xesteiras	99.30	0.1260	0.1610	99.18	0.0763	0.1057
Cariño	99.38	0.1252	0.1554	99.16	0.0770	0.1146
Salvora	99.31	0.1202	0.1581	99.19	0.0707	0.0998

Also, the adjustment degree of the estimated values for each instance of the testing dataset is shown in Appendix A (Figures A4–A6 and Figures A16–A18). As can be seen, the performance obtained was similar to that of the MLRs: R^2 was greater than 99%, and MAE and RMSE were lower than 0.10 and 0.15, respectively. Likewise, differences between the models of weather stations nearer or more distant from the case study were not detected, and identical results were obtained for the models of categories I and II. Apart from such similarity between the MLRs and MLPs of approach 1, there is a difference between both models that can limit the use of the MLPs: the size of the training dataset. As can be seen in Figure 9, the minimum size of a training dataset to obtain an acceptable performance is of 5 months, although increasing the training sample in 11–12 months would allow a greater stability in predictions to be guaranteed. In this sense, as can be proved in models of Table 8 (generated with a training dataset of 1 year), the performance of the estimations in the 675 days which composed the testing dataset was quite adjusted. Given that both the MLRs obtained similar performances and the minimum size of the training dataset for the MLRs is lower (1 month), the MLRs are therefore more possible to be used than the MLPs.

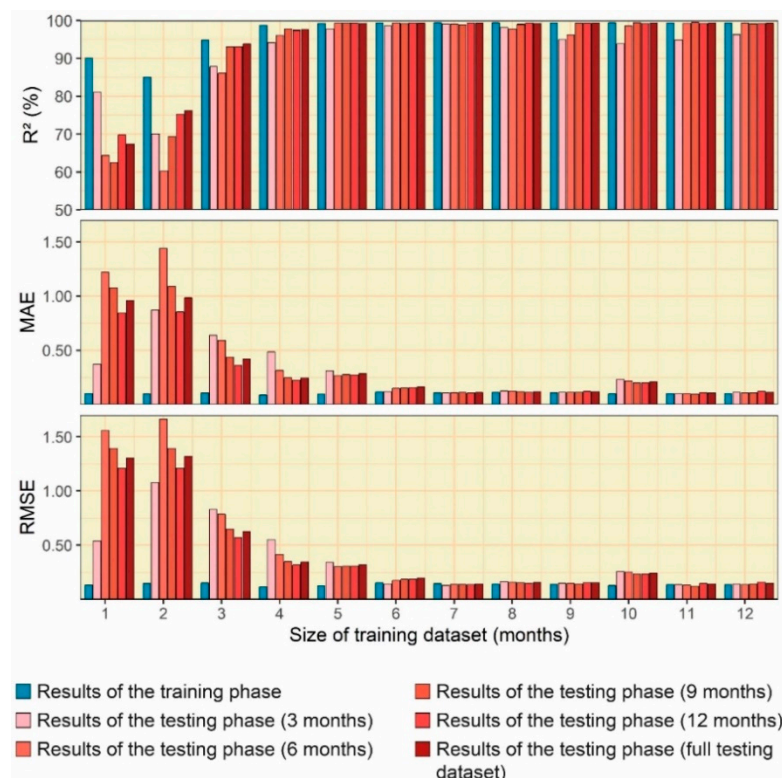


Figure 9. Influence of the size of the training sample on the MLP model (approach 1).

3.2. Approach 2: With Average Temperatures of the Last Seven Days

As mentioned in Section 2.3, this approach consisted of determining the adaptive setpoint temperature of the upper and lower limits by using external temperature data from the previous 7 days ($T_{ext,d-1}, T_{ext,d-2}, T_{ext,d-3}, T_{ext,d-4}, T_{ext,d-5}, T_{ext,d-6}, T_{ext,d-7}$). It was necessary to consider using the 7 external temperatures from the previous days because their performance improved for the MLR models (Figure 10) and the MLP models (Figure 11) by increasing the number of input variables.

3.2.1. MLR

As in the models of approach 1, the performance of the models of the different weather stations was first assessed for the adaptive setpoint temperatures of categories I, II, and III.

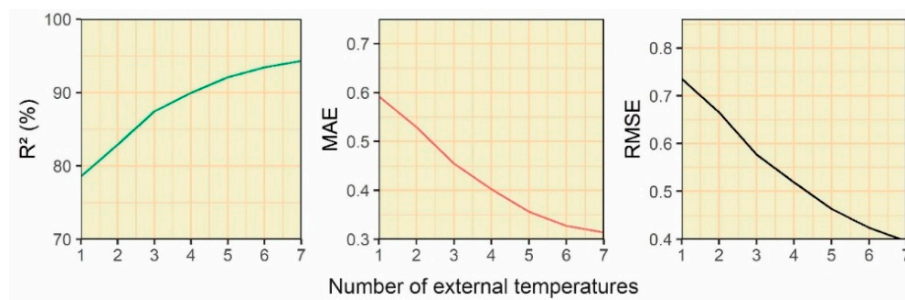


Figure 10. Influence of the number of the external temperatures used on the MLR model of A Gándara. Values obtained from the training of the model of the upper limit.

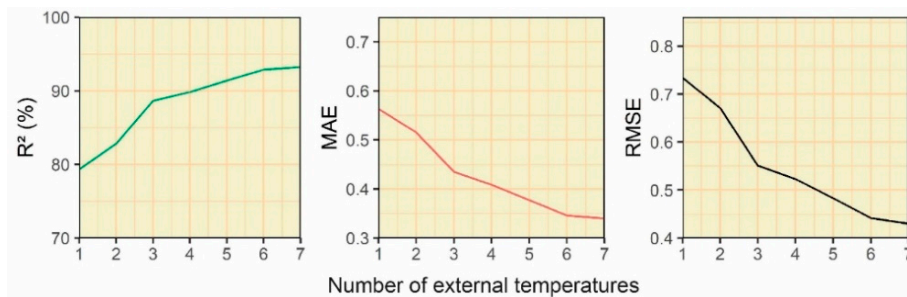


Figure 11. Influence of the number of the external temperatures used on the MLP model of A Gándara. Values obtained from the training of the model of the upper limit.

Results show that the models presented two different behaviours (Table 9): (i) on the one hand, the models for adaptive setpoint temperatures of the upper limit presented acceptable performances in some of the weather stations, with R^2 in the testing phase greater than 95% in most of the models, and values of MAE and $RMSE$ lower than 0.3 and 0.4, respectively. The worst estimations were when the running mean temperature presented values which were not within the applicability range of EN 15251 for the upper limit (in the case study analysed, values lower than 15 °C). In such cases, the estimation carried out by the model presented an error of 1 °C (see Appendix A). However, given that these cases are when using heating systems is required, the estimation for the upper limit is acceptable; and (ii) on the other hand, the models for the lower limit presented a low adjustment. In this sense, R^2 ranged between 81.60% and 87.45% in the training phase, and between 86.04% and 91.03% in the testing phase. Like for the upper limit, this was due to the difficulties of estimating both models for the days in that the running mean temperature was not within the applicability range for the lower limit. This aspect, together with the large number of instances (days) with values of static setpoint temperatures (202 days in the training dataset and 326 days in the testing dataset) made the obtaining of accurate results something of a challenge (Appendix A). The use of the MLRs with approach 2 was not therefore adequate to estimate the adaptive setpoint temperatures accurately.

3.2.2. MLP

The MLRs of approach 2 did not obtain acceptable results, so the performance that could be obtained with such approach was analysed by using the MLPs as a regression algorithm. Table 10 indicates the adequate performance presented by some of the models. Except the weather stations of Coruña-Bens, Rio do Sol, A Gándara, and Xesteiras, the remaining models obtained correlation coefficients greater than 95% in the training and testing phases in both limits, with acceptable error parameters. In this sense, MAE oscillated between 0.0800 and 0.1828, and $RMSE$ between 0.1236 and 0.2337 in the estimations of the setpoint temperatures of such models of the upper limit (see Figures A10–A12) and the lower limit (see Figures A22–A24). These values allowed estimations to be carried out with an adequate adjustment degree of the adaptive setpoint temperatures of the upper and lower limits.

Table 9. Results of the training and testing of the MLR models of approach 2.

Model	Upper Limit			Lower Limit		
	R^2	MAE	RMSE	R^2	MAE	RMSE
Training						
Coruña-Hercules	98.20	0.1621	0.2251	85.25	0.2865	0.3490
Coruña-Bens	97.97	0.1747	0.2389	86.03	0.2835	0.3404
Rio do Sol	94.04	0.3138	0.4057	83.03	0.2965	0.3721
A Gándara	94.42	0.3026	0.3930	83.25	0.2947	0.3699
Coto Muiño	98.44	0.1523	0.2100	87.45	0.2686	0.3238
Santiago EOAS	97.69	0.1952	0.2548	87.31	0.2637	0.3255
Sambreixo	97.96	0.1843	0.2398	87.11	0.2688	0.3279
Xesteiras	90.88	0.3859	0.4978	81.60	0.2993	0.3860
Cariño	97.00	0.2173	0.2903	87.06	0.2652	0.3285
Salvora	98.20	0.1621	0.2251	85.25	0.2865	0.3490
Testing						
Coruña-Hercules	97.35	0.2039	0.3017	86.04	0.3300	0.3884
Coruña-Bens	96.91	0.4471	0.5543	91.03	0.2769	0.3434
Rio do Sol	97.71	0.2640	0.3171	88.17	0.3089	0.3669
A Gándara	97.52	0.2830	0.3354	88.62	0.3053	0.3643
Coto Muiño	98.75	0.1581	0.2086	89.83	0.2805	0.3376
Santiago EOAS	98.39	0.1884	0.2333	89.13	0.2914	0.3430
Sambreixo	98.34	0.1684	0.2267	87.78	0.2986	0.3621
Xesteiras	95.40	0.3482	0.4116	86.79	0.3200	0.3853
Cariño	98.13	0.1925	0.2619	87.89	0.2998	0.3623
Salvora	97.35	0.2039	0.3017	86.04	0.3300	0.3884

Table 10. Results of the training and testing of the MLP models of approach 2.

Model	Upper Limit			Lower Limit		
	R^2	MAE	RMSE	R^2	MAE	RMSE
Training						
Coruña-Hercules	98.86	0.1376	0.1805	97.81	0.0950	0.1393
Coruña-Bens	97.29	0.2280	0.2869	96.24	0.1343	0.1862
Rio do Sol	93.47	0.3336	0.4263	87.31	0.2330	0.3280
A Gándara	94.02	0.3501	0.4483	86.99	0.2365	0.3339
Coto Muiño	98.97	0.1350	0.1716	97.91	0.0969	0.1362
Santiago EOAS	97.19	0.2204	0.2810	94.88	0.1507	0.2136
Sambreixo	98.23	0.1799	0.2278	97.12	0.1105	0.1600
Xesteiras	88.74	0.4402	0.5521	82.40	0.2803	0.3849
Cariño	96.92	0.2266	0.295	95.23	0.1293	0.2046
Salvora	98.86	0.1376	0.1805	97.81	0.0950	0.1393
Testing						
Coruña-Hercules	98.52	0.1551	0.221	98.09	0.1031	0.1643
Coruña-Bens	96.77	0.4797	0.6048	96.58	0.3583	0.5248
Rio do Sol	97.43	0.2303	0.2861	94.24	0.1947	0.2827
A Gándara	97.06	0.2362	0.3004	93.96	0.1470	0.2594
Coto Muiño	99.03	0.1417	0.1865	98.70	0.0800	0.1236
Santiago EOAS	98.59	0.1677	0.2148	98.19	0.1187	0.1597
Sambreixo	98.94	0.1755	0.2282	98.30	0.1270	0.1647
Xesteiras	95.17	0.3259	0.3949	91.66	0.2244	0.3203
Cariño	98.46	0.1828	0.2337	97.09	0.1374	0.1903
Salvora	98.52	0.1551	0.221	98.09	0.1031	0.1643

A better estimation obtained by the MLPs was not detected either in those weather stations presenting similar temperature distributions because the correlation coefficients greater than 98% were obtained in the testing phase of the weather stations located in areas with a height difference of more than 200 m, such as Coto Muiño, Santiago EOAS, and Sambreixo. Given that the MLPs obtained adequate results by using approach 2, the minimum size of the training dataset was analysed as in the models of approach 1. The performances obtained by increasing the number of months included in the

training dataset are represented in Figure 12. As can be seen, the performance of the MLP presented acceptable behaviour when the training dataset included data of 6 months. Such minimum size is the same as that obtained in the MLP of approach 1, so it is shown again the need for having large training datasets to carry out estimations of the adaptive setpoint temperatures accurately.

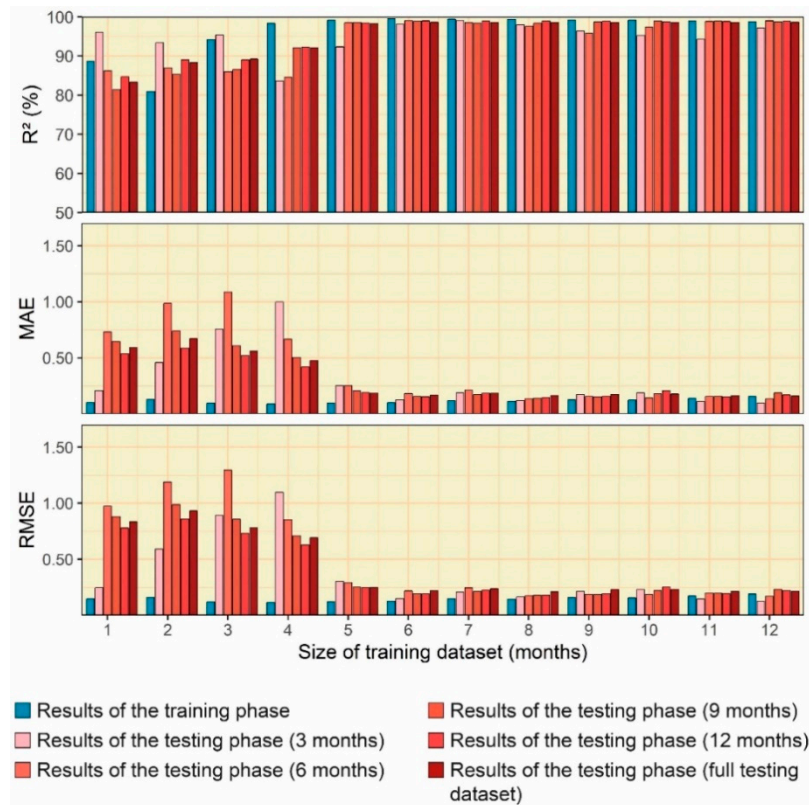


Figure 12. Influence of the size of the training sample on the MLP model (approach 2).

3.3. Estimation Methodology of the Adaptive Setpoint Temperatures

Based on the results obtained of approaches 1 and 2, the use of MLRs and MLPs allowed the adaptive setpoint temperatures to be accurately estimated. According to the approach used, the regression algorithm presented different behaviour: whereas the MLRs and the MLPs can be used for approach 1, only the use of the MLPs obtained adequate results for approach 2.

The existing differences between the input variables of both approaches imply many possibilities of being used. In this sense, one of such possibilities of using the methods suggested is the configuration of the thermostat of the HVAC system to estimate the setpoint temperature if the external temperature sensor fails (Figure 13). By connecting the thermostat to internet, the data obtained from the weather stations of the meteorological agency of the area (in the present case study, MeteoGalicia) have been imported to generate the data vector to be introduced into the models in order to estimate the adaptive setpoint temperature. Because of possible lacks in the data records (e.g., the setpoint temperature from the previous day has not been recorded or some weather stations fail), the use of both approaches and data from various weather stations (e.g., 5 weather stations) would guarantee the correct estimation of the adaptive setpoint temperatures. If all models can carry out the estimation correctly due to the accuracy obtained in the estimations of the models, the final output value can be obtained by means of the average of the different adaptive setpoint temperatures obtained. This methodology could be used if the external temperature probe fails or in case such probe has been removed because it fails, and another probe cannot be installed. It could also be used if an external temperature probe is provisionally installed in the HVAC system. The probe would be removed when a minimum training size is available to generate the MLRs models of approach 1 (i.e., measurements of 1 month).

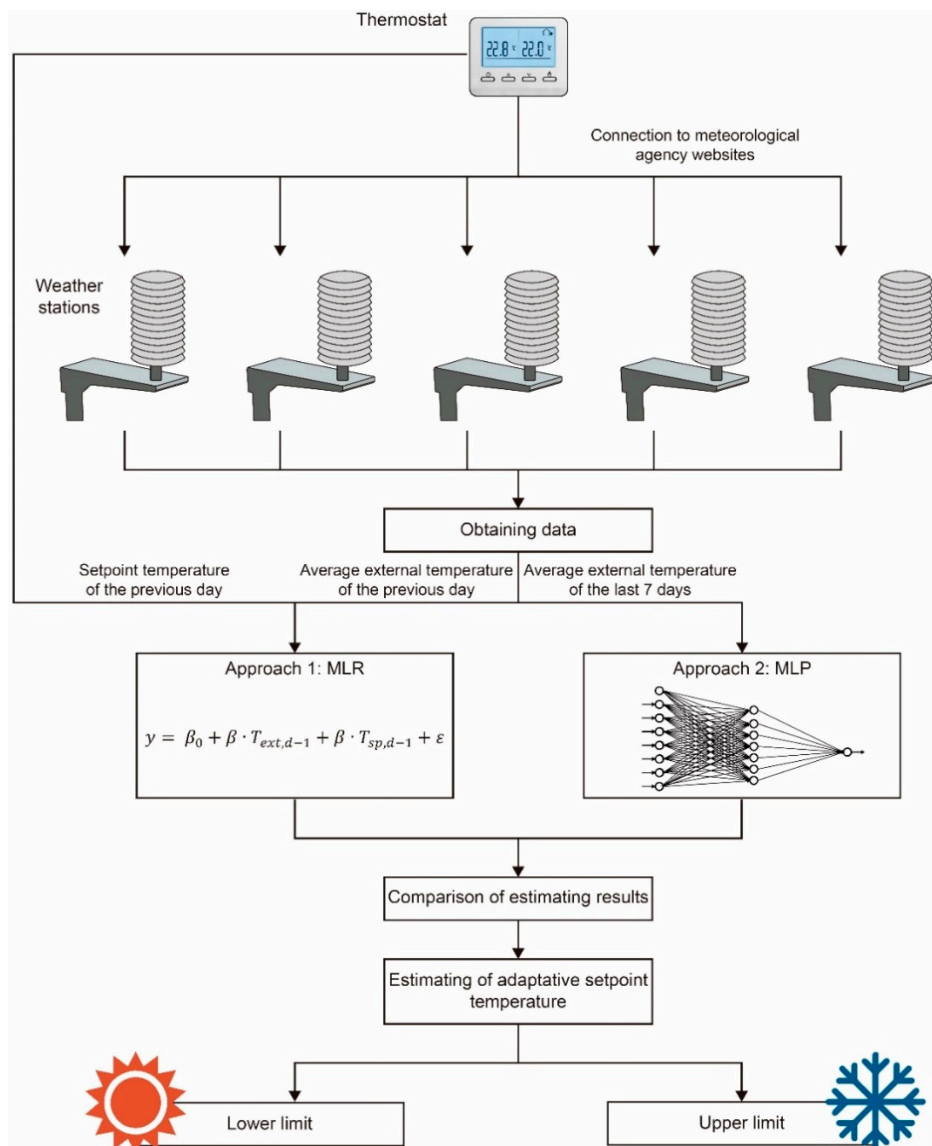


Figure 13. Estimation methodology of adaptive setpoint temperatures. Failures in the external temperature probe or temporary installation are considered.

Also, another great possibility to be used is related to approach 2. Unlike approach 1, the MLPs of approach 2 estimated the adaptive setpoint temperatures using only external temperature data. Considering this aspect, configurations of adaptive setpoint temperatures could be implemented in HVAC systems without the need of having external temperature probes, thereby reducing the economic cost of implementing such energy conservation measures, contributing to a high implementation rate, and avoiding possible errors caused by distortions in the measurement of the external temperature during its operation. Therefore, local MLPs could be developed for the different cities or climate zones of a country by using data from weather stations to be used by buildings located in such areas. Like in the methodology shown in Figure 13, the thermostat would be connected to the weather stations of the meteorological agency, and the average values of the external temperature from the previous 7 days would be imported and then introduced into the MLP of each weather station to estimate the adaptive setpoint temperatures (see Figure 14).

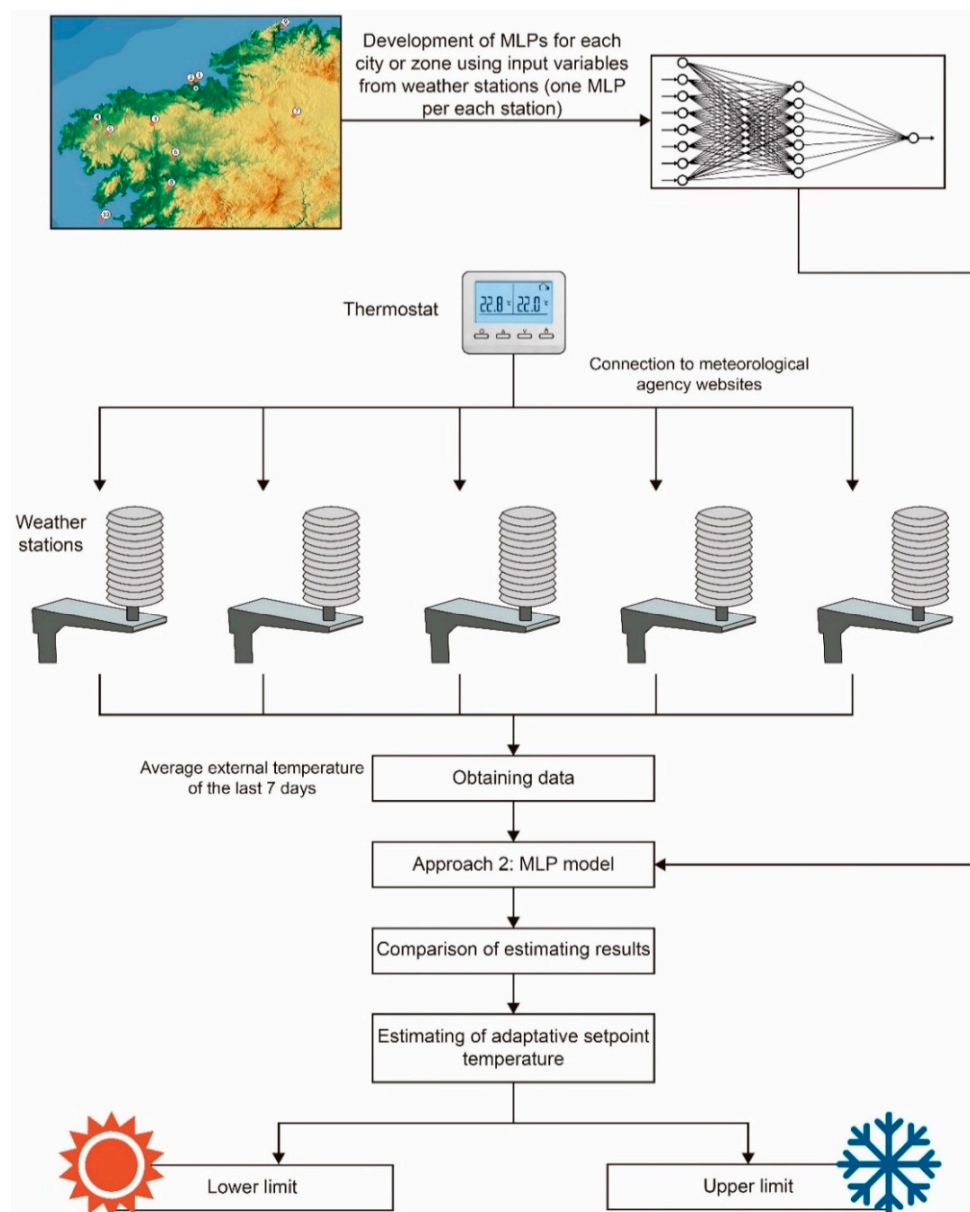


Figure 14. Estimation methodology of adaptive setpoint temperatures. Not using external temperature probes is considered.

4. Conclusions

Due to the limitations presented by the implementation of adaptive setpoint temperatures (it should be determined according to the variations of the external temperature), various possibilities of determining such typology of setpoint temperatures without measuring the external temperature are studied in this paper. To achieve this, two approaches were analysed by using two different regression algorithms: a multivariable linear regression and a multilayer perceptron. The approaches were different because of the type of input variables used by each: approach 1 used the setpoint temperature from the previous day and the mean daily external temperature from the previous day, and approach 2 used the mean daily external temperature from the previous 7 days. External temperature data were obtained from 10 weather stations of the meteorological agency MeteoGalicia, which were located at different heights and areas distant from the case study. This allowed the reliability of using the method with data from other climate zones to be ensured.

Based on the results obtained with a dataset of 1040 days, the conclusions are as follows:

- The approach which used the values of setpoint temperature and mean daily external temperature from the previous day to estimate adaptive setpoint temperatures carried out estimations close to the actual values by using both data from all weather stations and two regression algorithms. In this way, the only difference between such algorithms was the time required to generate models with an adequate performance (1 month for the multivariable linear regression models and 5 months or more for multilayer perceptrons). This is useful to guarantee the feasibility of using MLRs to carry out estimations with an appropriate degree of accuracy.
- The approach which used the average values of the external temperature from the previous 7 days had different behaviour with respect to the other approach: only multilayer perceptrons obtained adequate performances, whereas the multivariable linear regression models obtained low correlation coefficients both in the training and testing phases. This was due to the limitations presented by the multivariable linear regression models when the adaptive setpoint temperatures were estimated not within the applicability of EN 15251 in the intervals of the running mean temperature. However, this aspect did not decrease the accuracy of the estimations carried out using the multilayer perceptrons, and accurate models could be obtained with training datasets of at least 6 months.

The results of this research could be useful for energy auditors, engineers, architects, installers, and construction companies because new and existing buildings could be provided with HVAC systems with a lower energy consumption. Firstly, the two approaches would ensure the continuity of using adaptive setpoint temperatures despite possible measurement errors or failures of the external temperature probes. Secondly, the possibility of developing multilayer perceptrons carrying out estimations by using measurements from weather stations of the official meteorological agencies in the country or region would implement adaptive systems both in the existing equipment in the building stock and buildings where the installation of external temperature probes is not recommended (e.g., façades facing west and with a strong incidence of solar radiation). This research could therefore improve the energy efficiency of the building stock, and adaptive setpoint systems could be implemented in many existing buildings in the medium term. Given that the methodology proposed has not been applied to a real case study, further steps of this research will be focused on its use in a dwelling.

Author Contributions: All the authors contributed equally to this work. All the authors participated in preparing the research from the beginning to end, such as establishing the research design, method, and analysis. All the authors discussed and finalized the analysis results to prepare the manuscript in accordance with the research progress. All the authors have read and approved the final manuscript.

Funding: This work was partially supported by the Spanish Ministry of Science, Innovation and Universities (Code 00064742/ITC-20133094), funded by CDTI (Centro para el Desarrollo Tecnológico e Industrial) under the FEDER-Innterconecta Program, and co-financed with European Union Regional Development Fund. Also, was partially supported by Spanish Ministry of Economy, Industry and Competitiveness (Code BIA 2017-85657-R).

Acknowledgments: The authors would like to acknowledge “Plan Propio de Investigación de la Universidad de Sevilla (IV.11. Acciones especiales convocatoria 2018)” for financing the mobility of David Bienvenido-Huertas at the University of a Coruña.

Conflicts of Interest: The authors declare no conflict of interest.

Appendix A

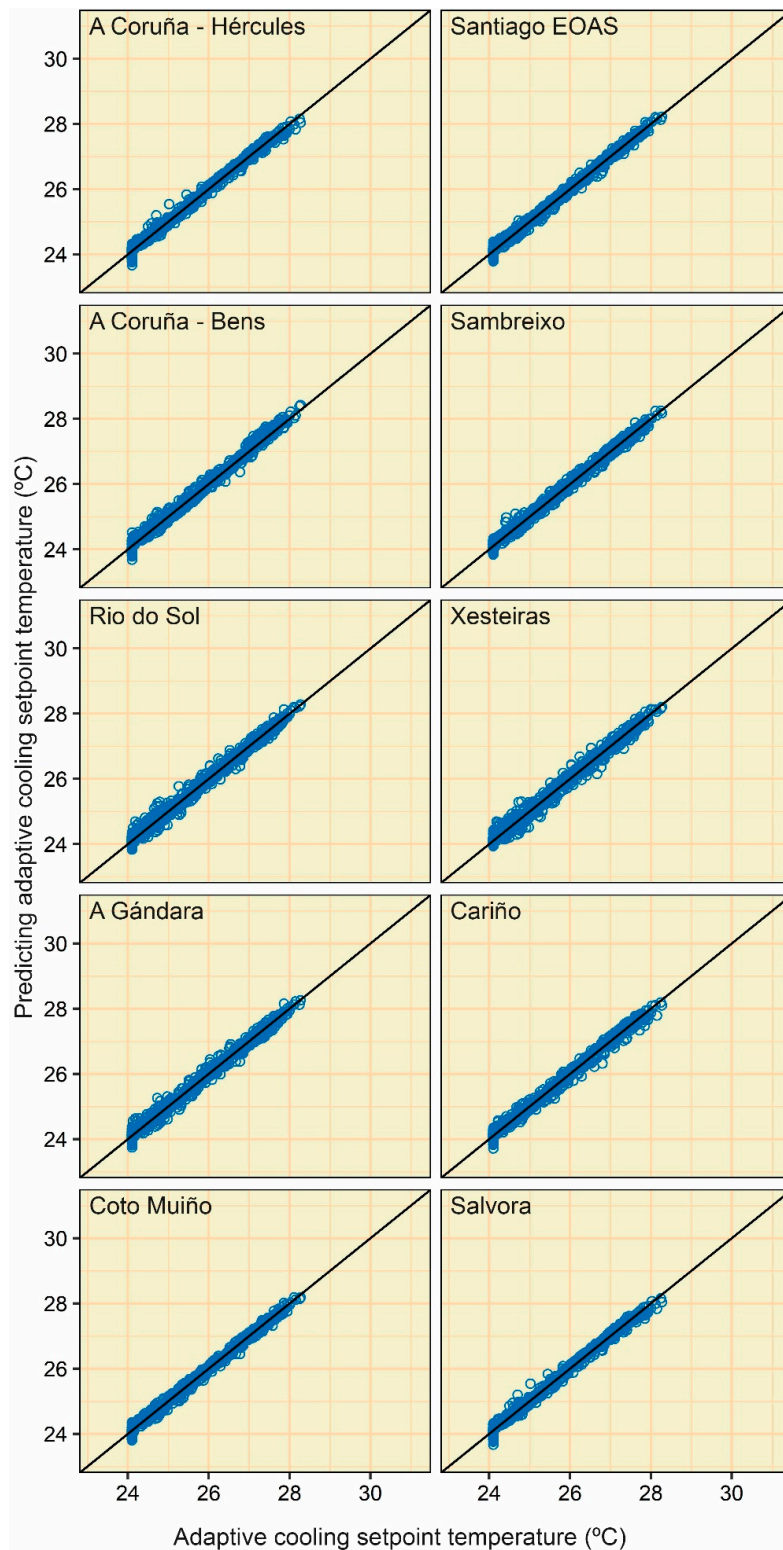


Figure A1. Point clouds between the actual and predicting adaptive cooling setpoint temperature values (category I) of the MLR (approach 1).

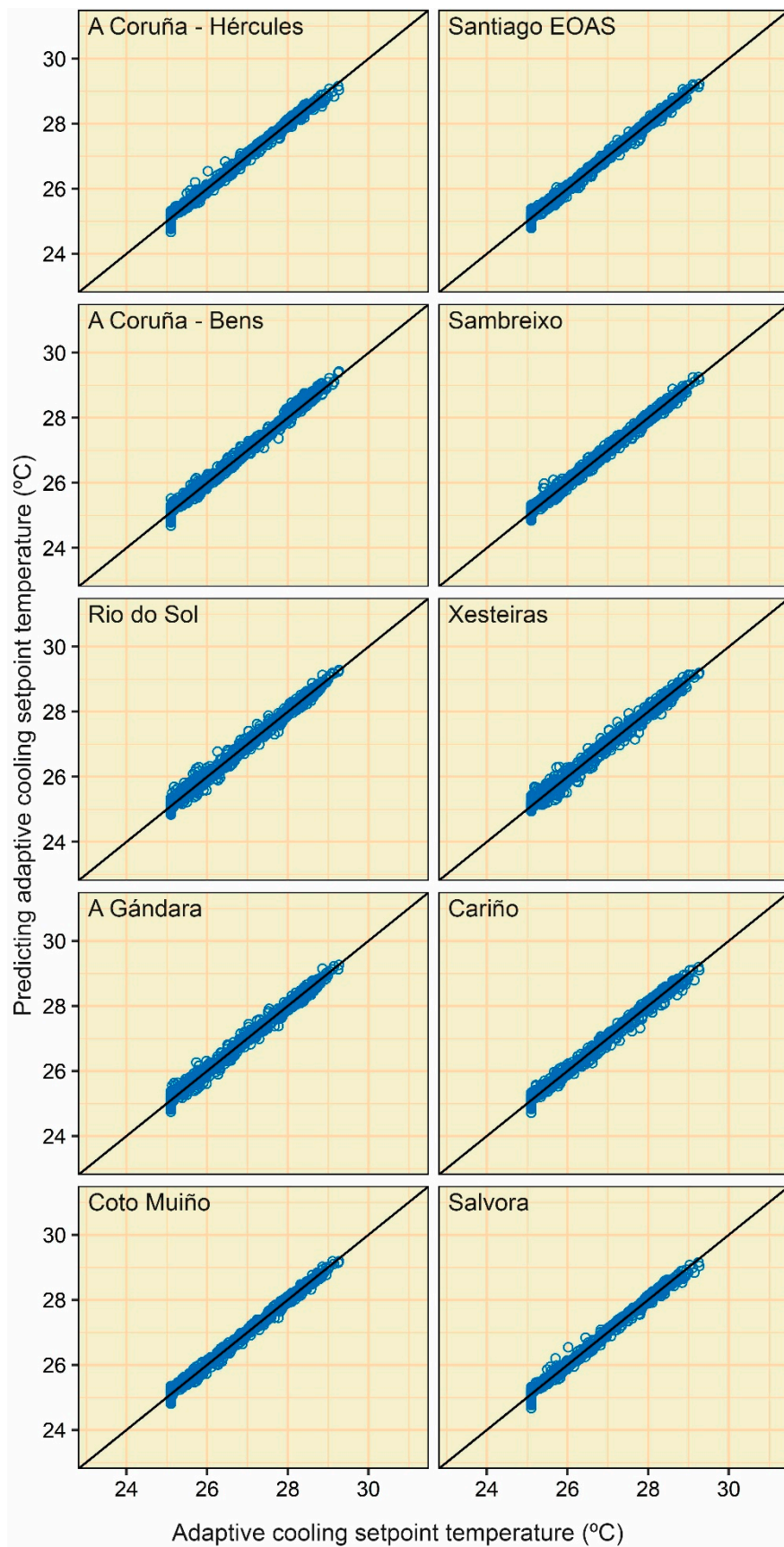


Figure A2. Point clouds between the actual and predicting adaptive cooling setpoint temperature values (category II) of the MLR (approach 1).

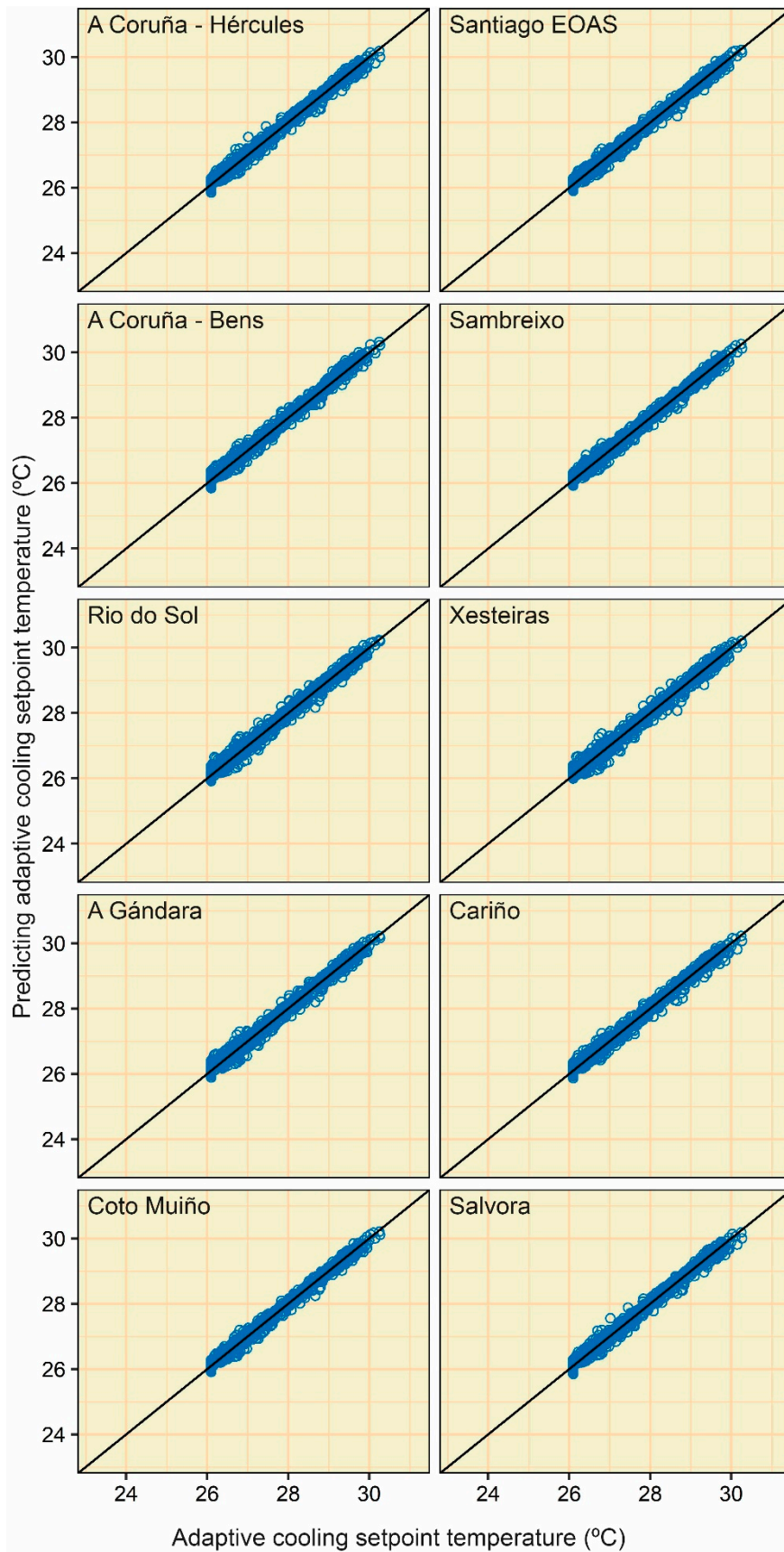


Figure A3. Point clouds between the actual and predicting adaptive cooling setpoint temperature values (category III) of the MLR (approach 1).

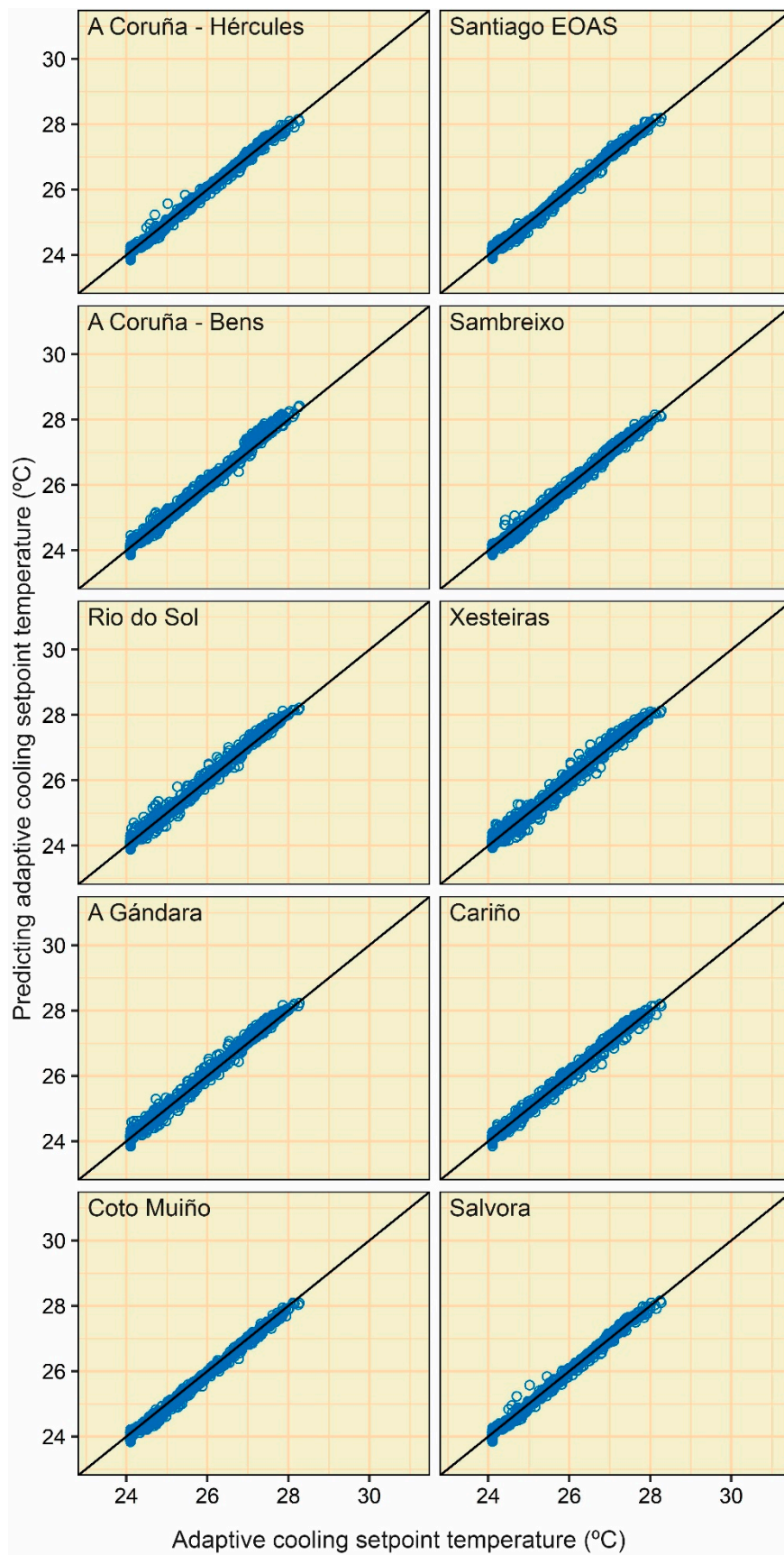


Figure A4. Point clouds between the actual and predicting adaptive cooling setpoint temperature values (category I) of the MLP (approach 1).

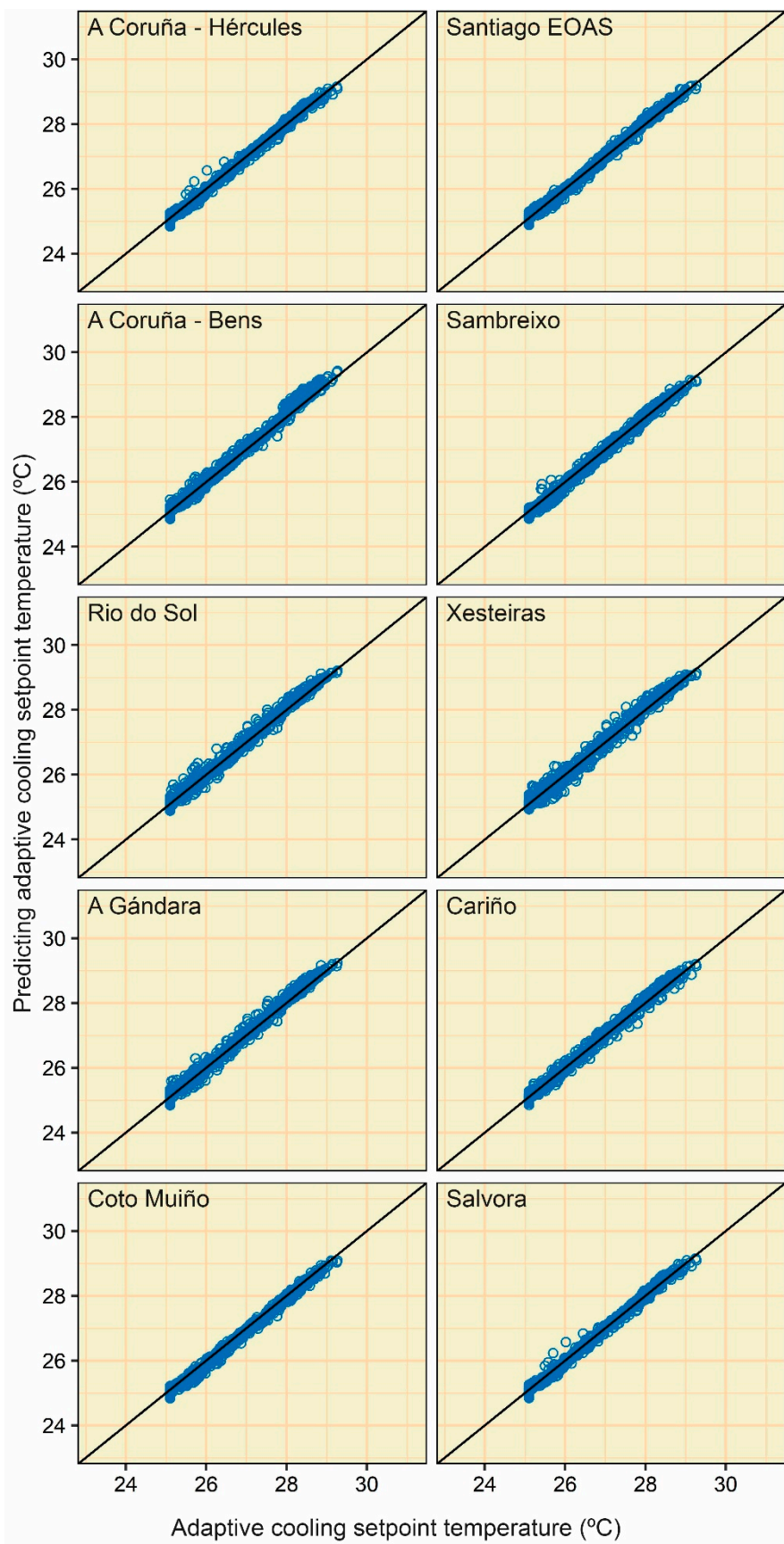


Figure A5. Point clouds between the actual and predicting adaptive cooling setpoint temperature values (category II) of the MLP (approach 1).

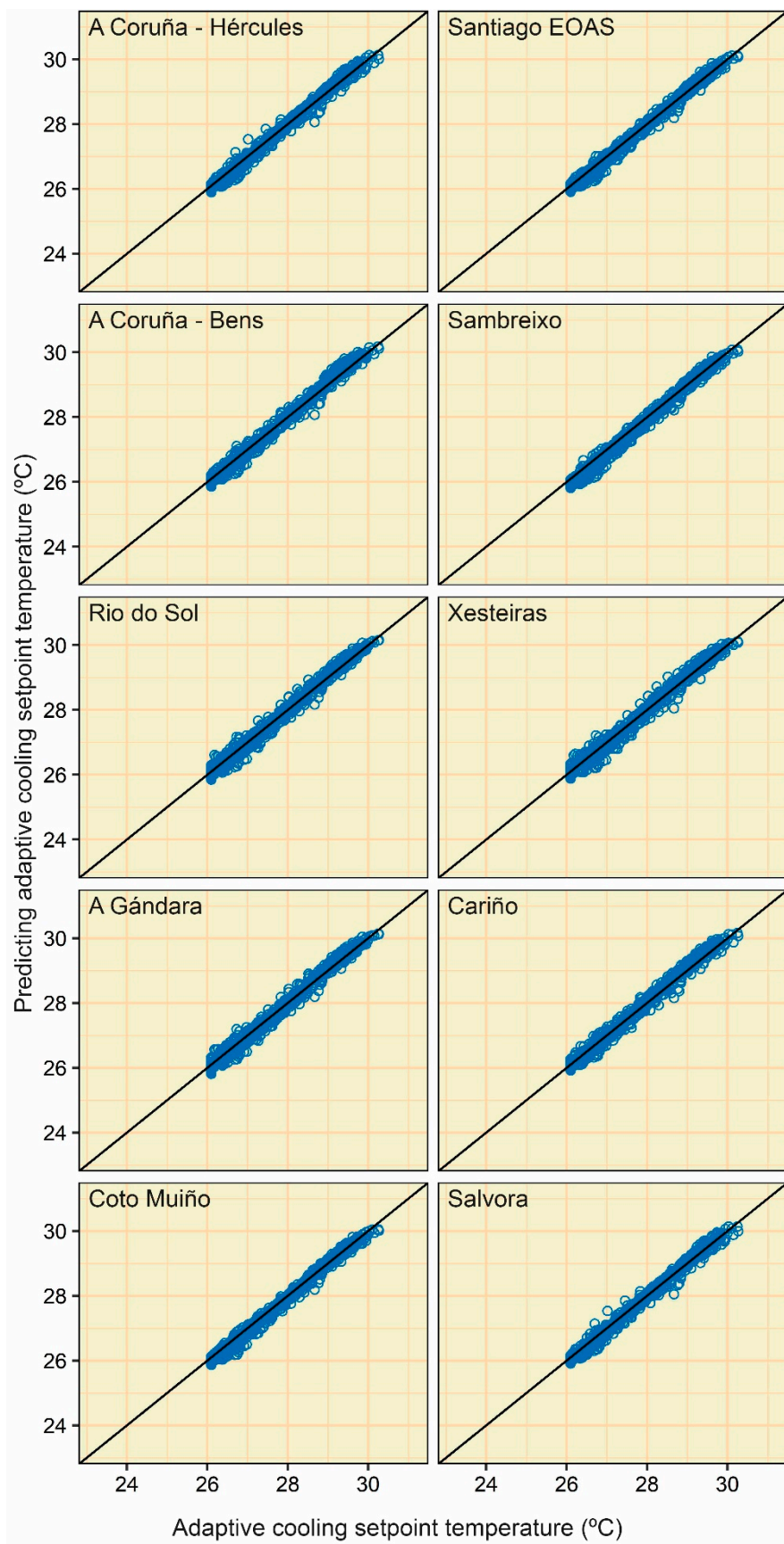


Figure A6. Point clouds between the actual and predicting adaptive cooling setpoint temperature values (category III) of the MLP (approach 1).

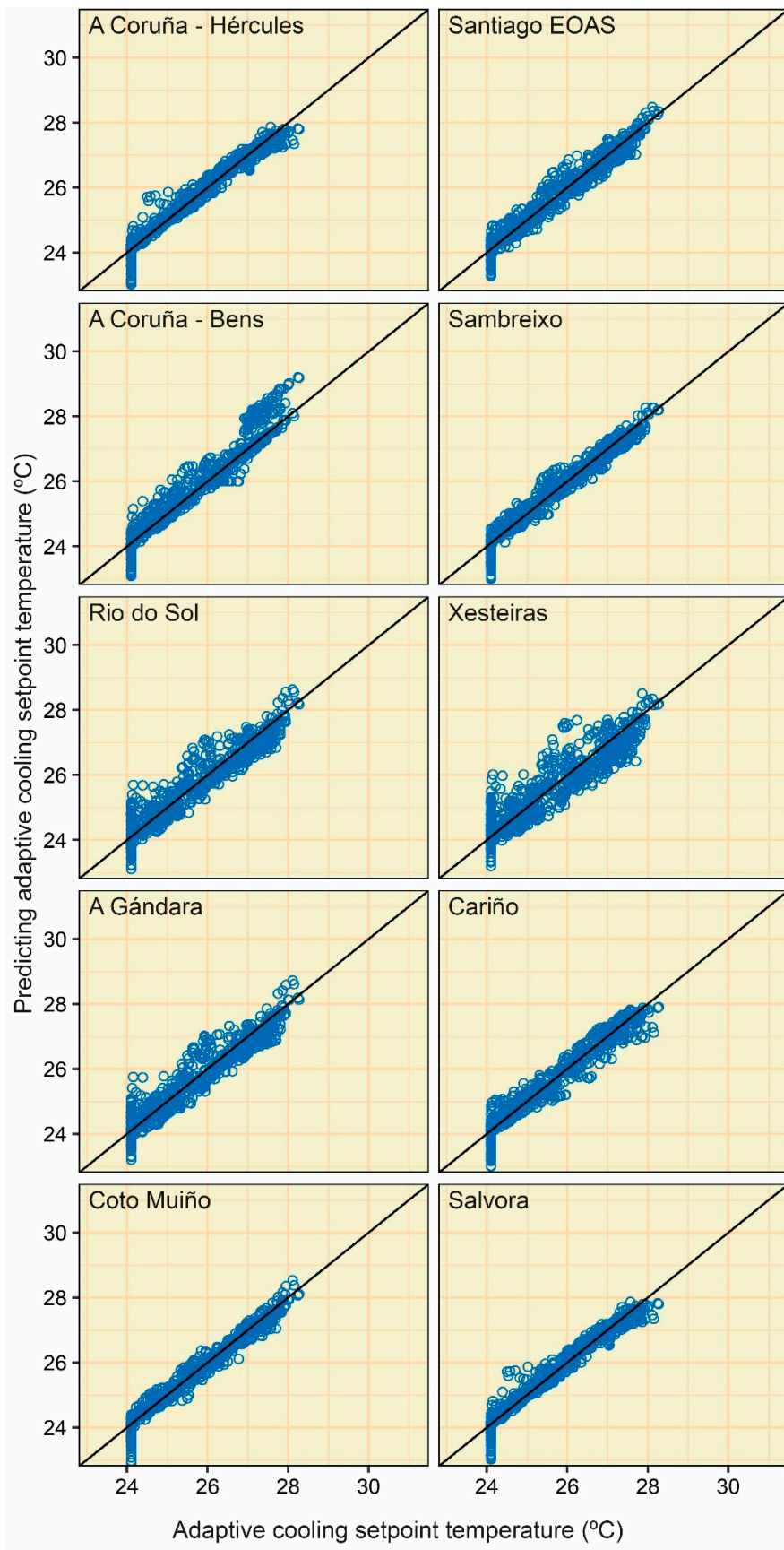


Figure A7. Point clouds between the actual and predicting adaptive cooling setpoint temperature values (category I) of the MLR (approach 2).

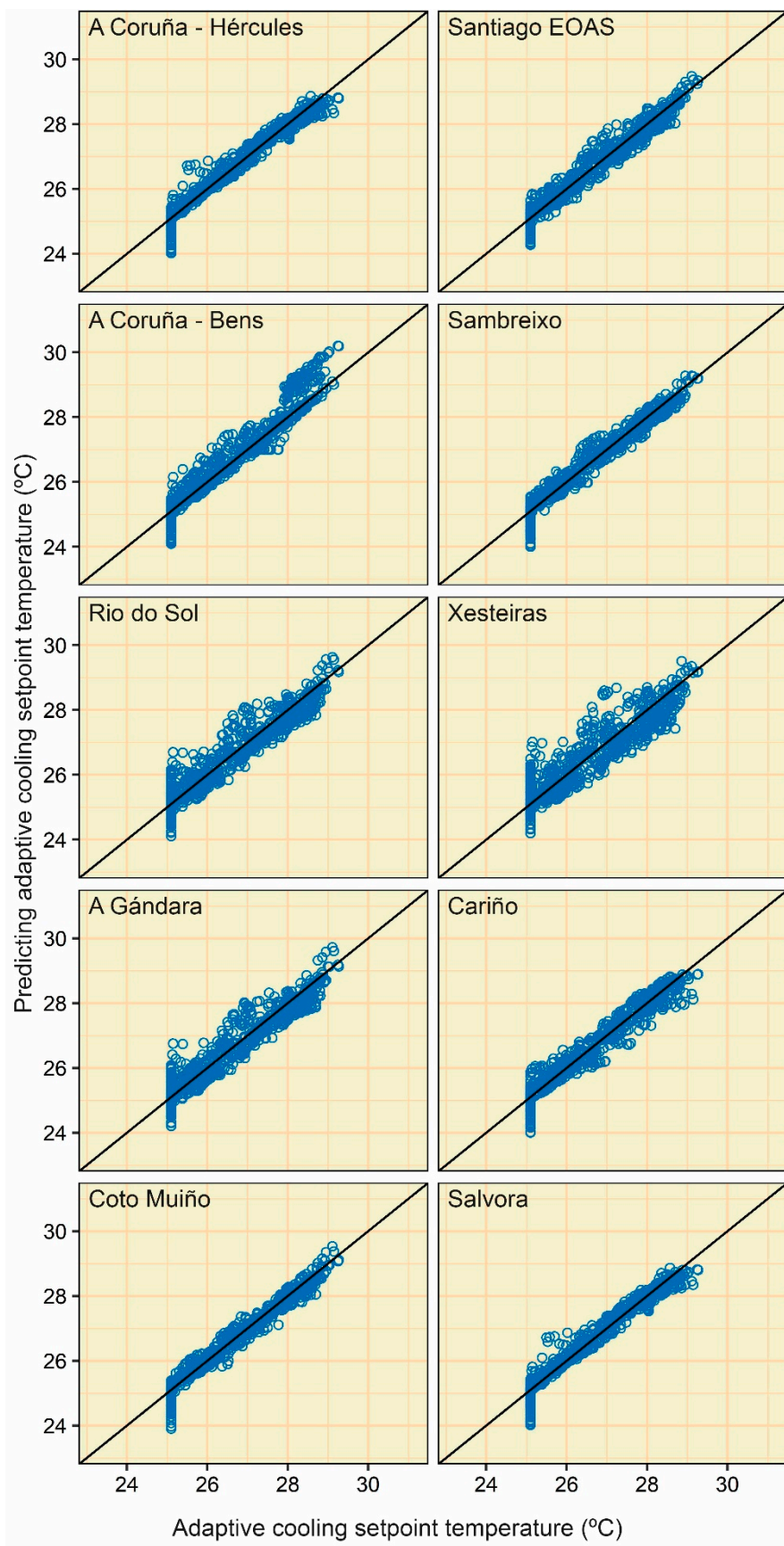


Figure A8. Point clouds between the actual and predicting adaptive cooling setpoint temperature values (category II) of the MLR (approach 2).

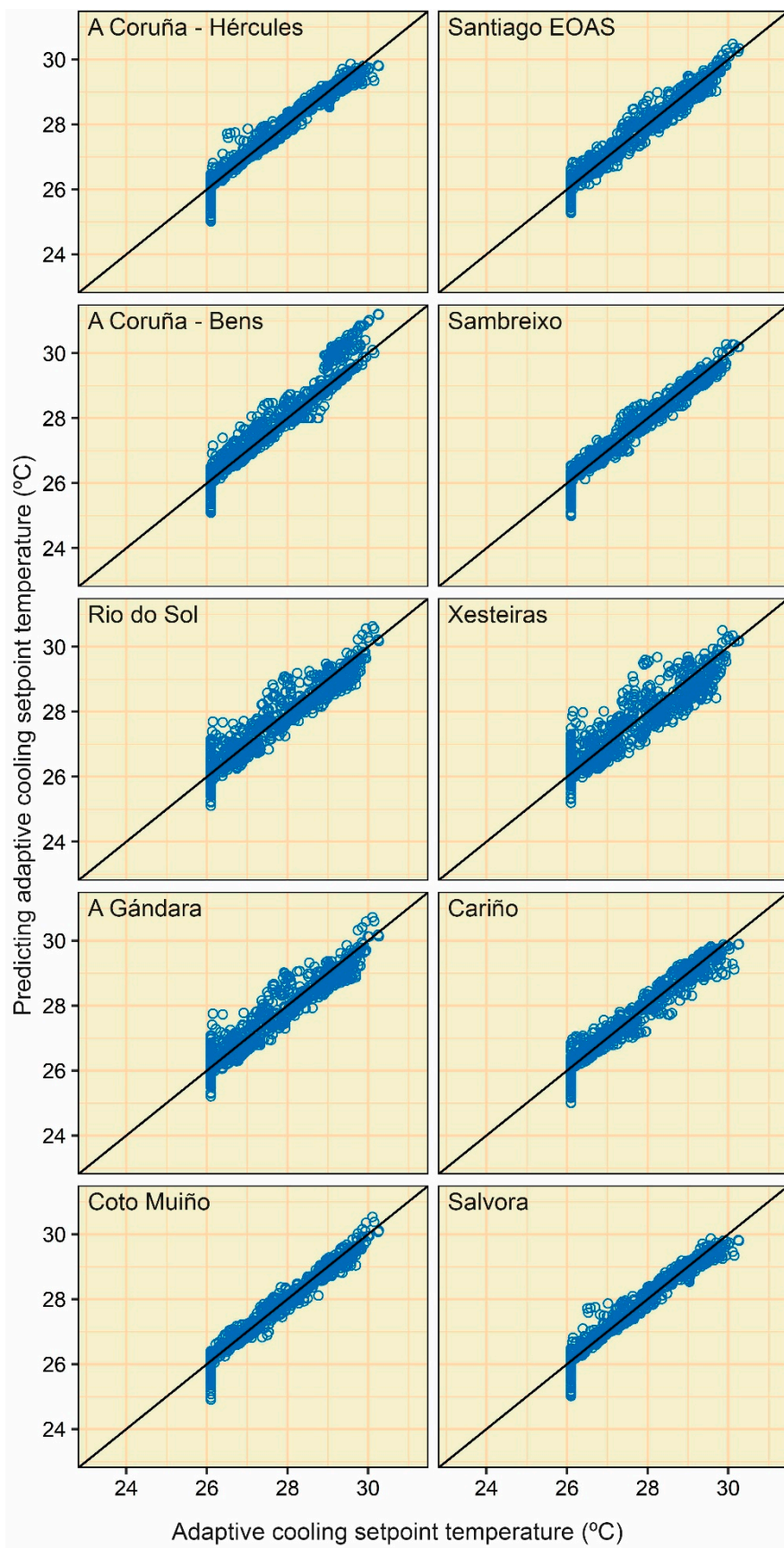


Figure A9. Point clouds between the actual and predicting adaptive cooling setpoint temperature values (category III) of the MLR (approach 2).

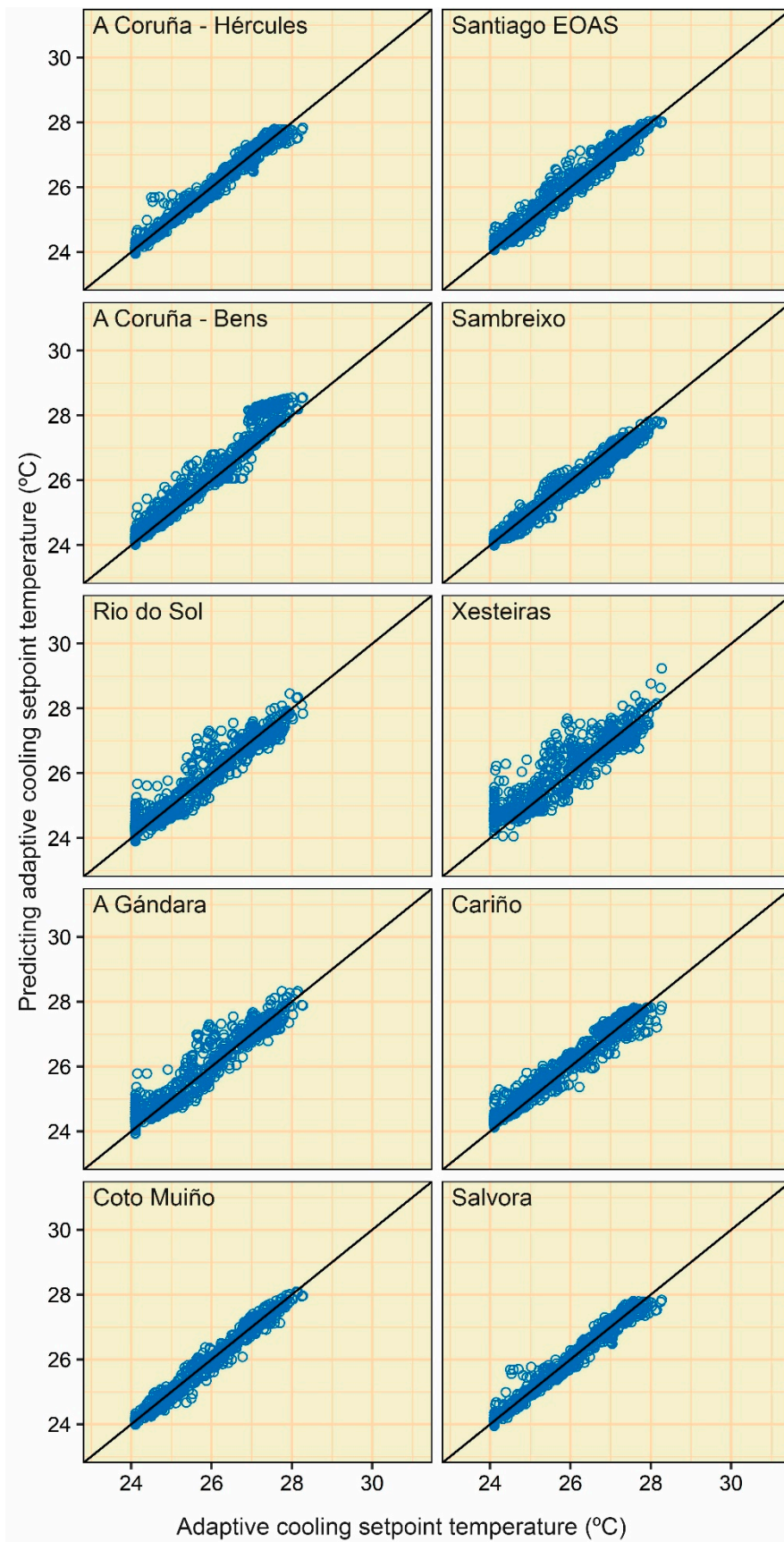


Figure A10. Point clouds between the actual and predicting adaptive cooling setpoint temperature values (category I) of the MLP (approach 2).

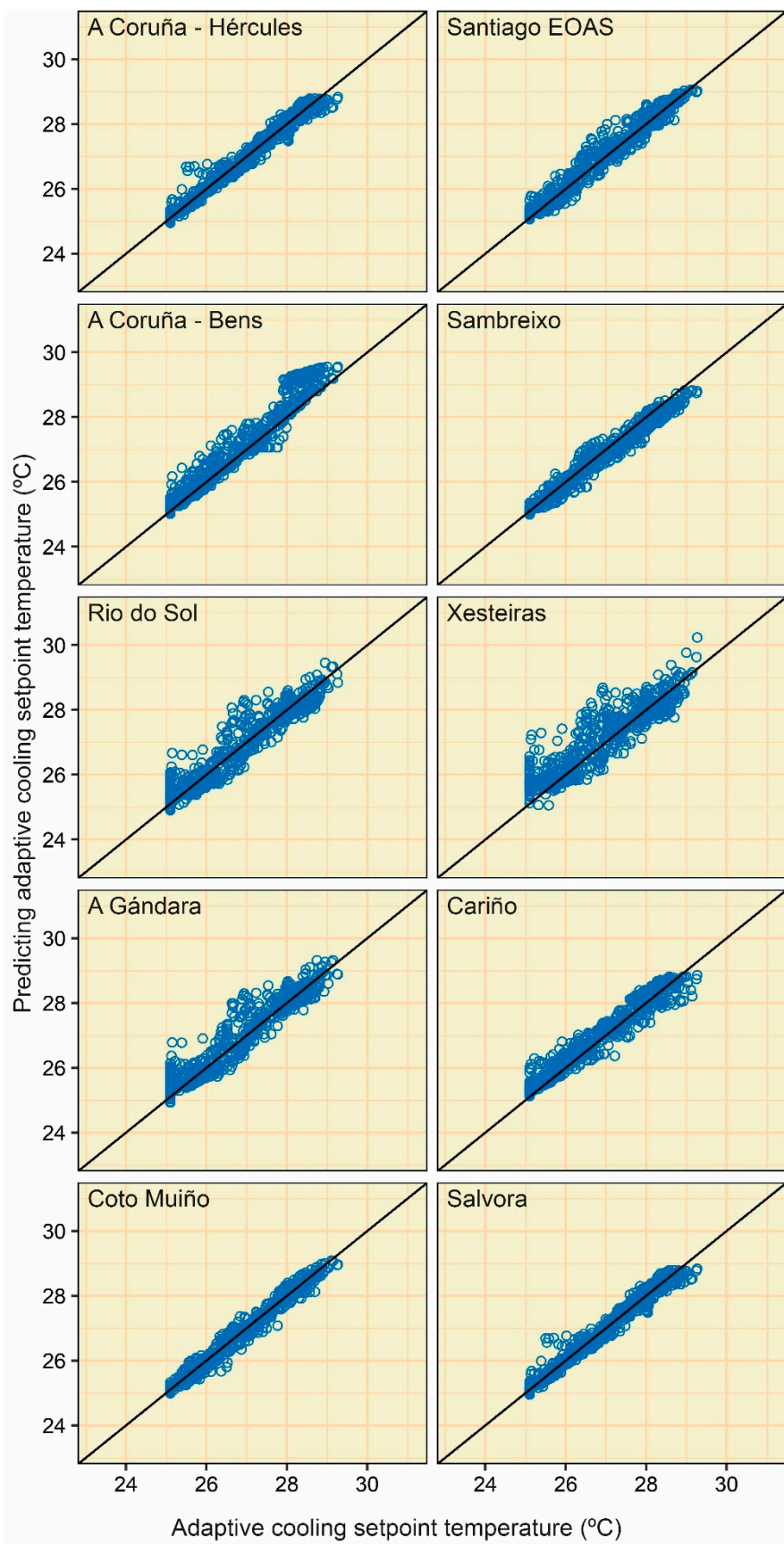


Figure A11. Point clouds between the actual and predicting adaptive cooling setpoint temperature values (category II) of the MLP (approach 2).

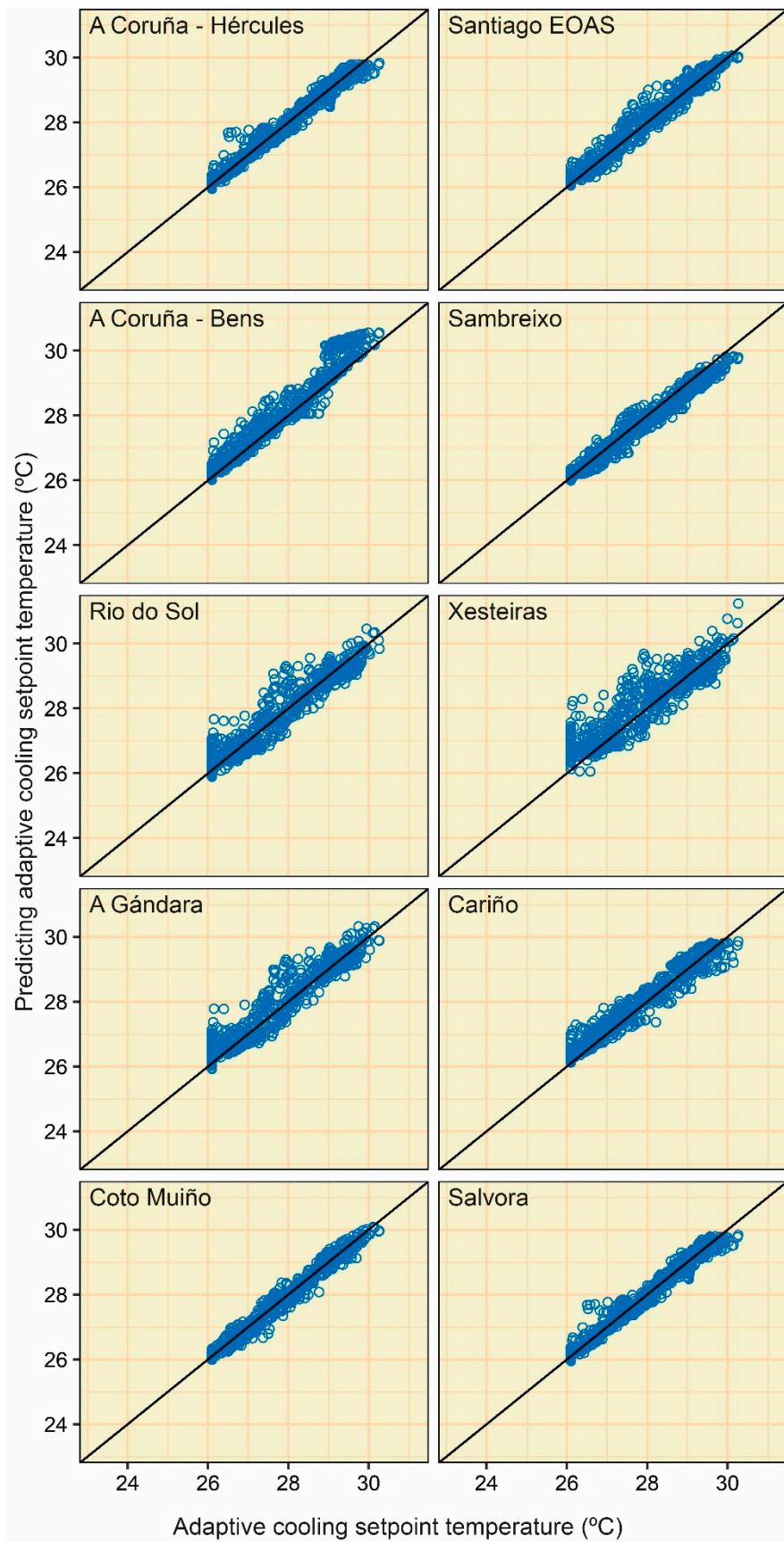


Figure A12. Point clouds between the actual and predicting adaptive cooling setpoint temperature values (category III) of the MLP (approach 2).

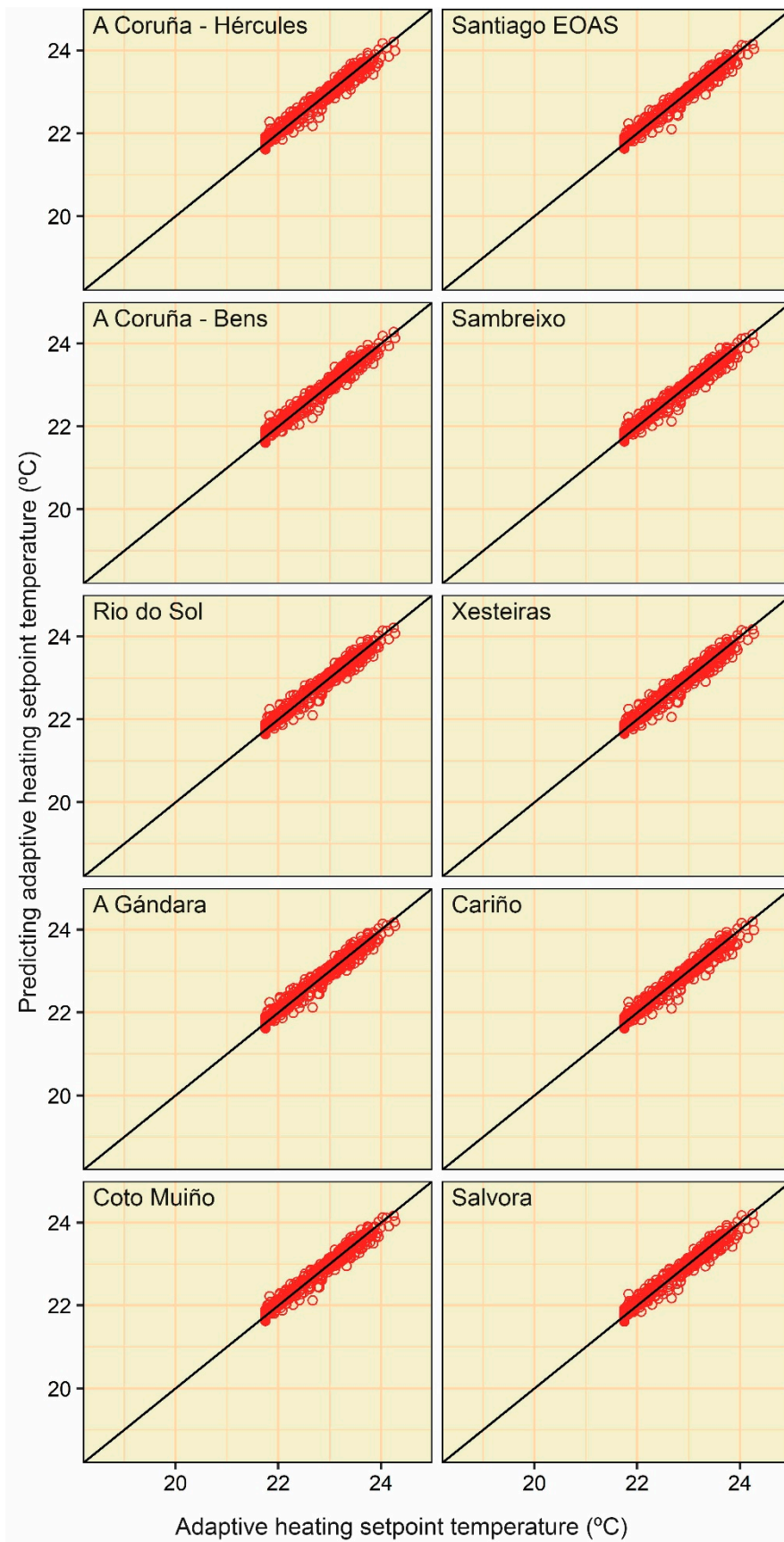


Figure A13. Point clouds between the actual and predicting adaptive heating setpoint temperature values (category I) of the MLR (approach 1).

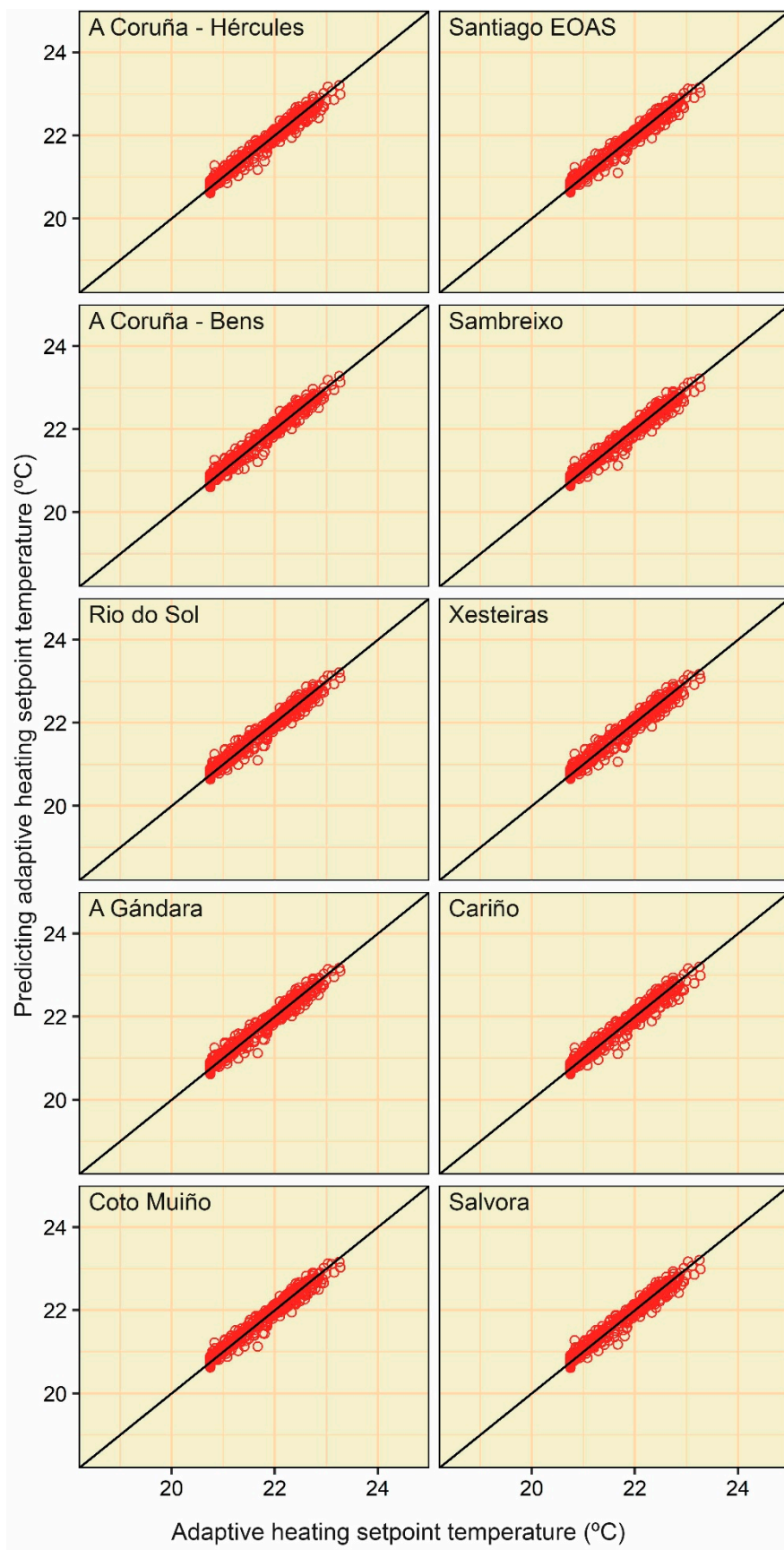


Figure A14. Point clouds between the actual and predicting adaptive heating setpoint temperature values (category II) of the MLR (approach 1).

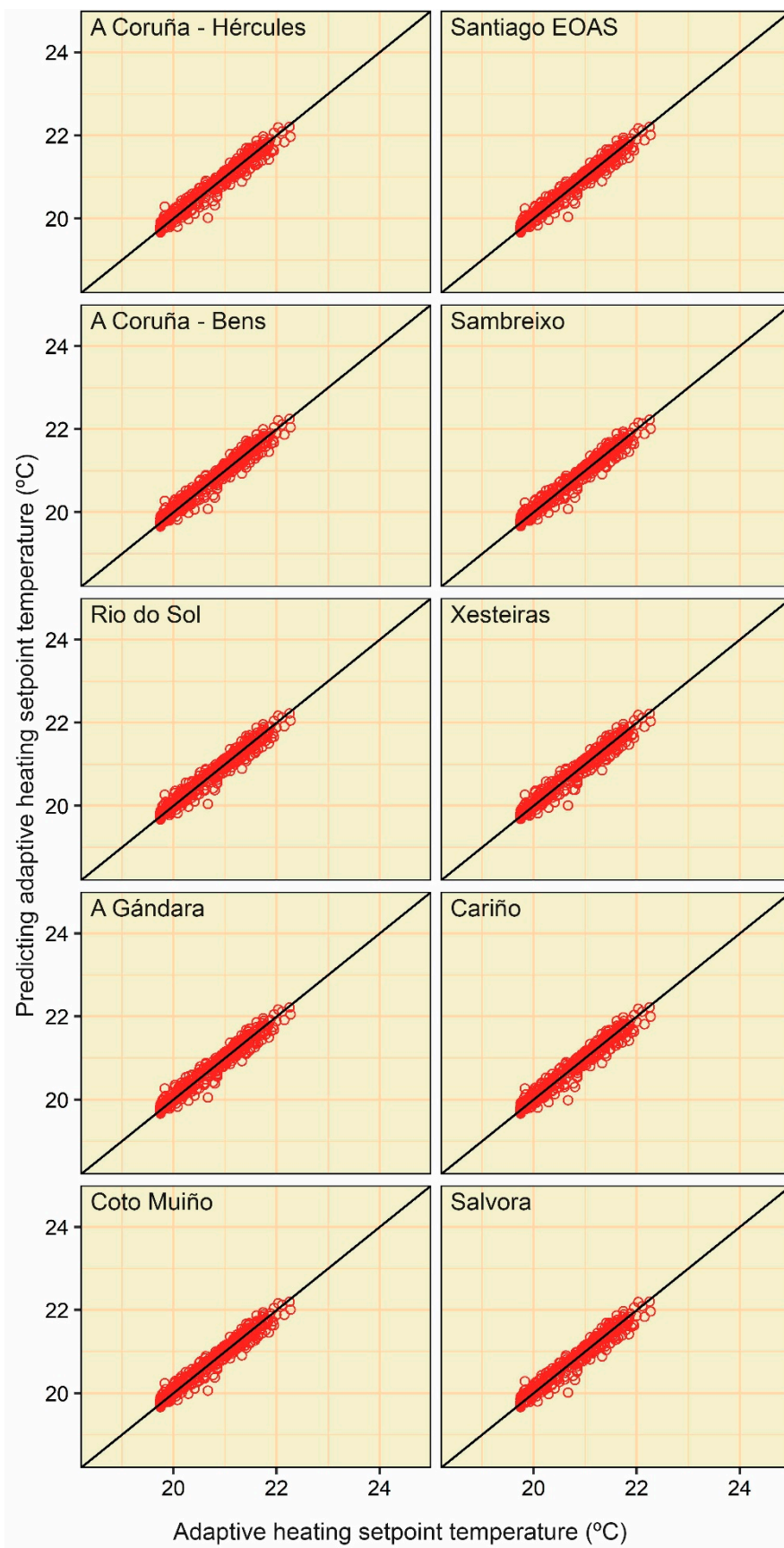


Figure A15. Point clouds between the actual and predicting adaptive heating setpoint temperature values (category III) of the MLR (approach 1).

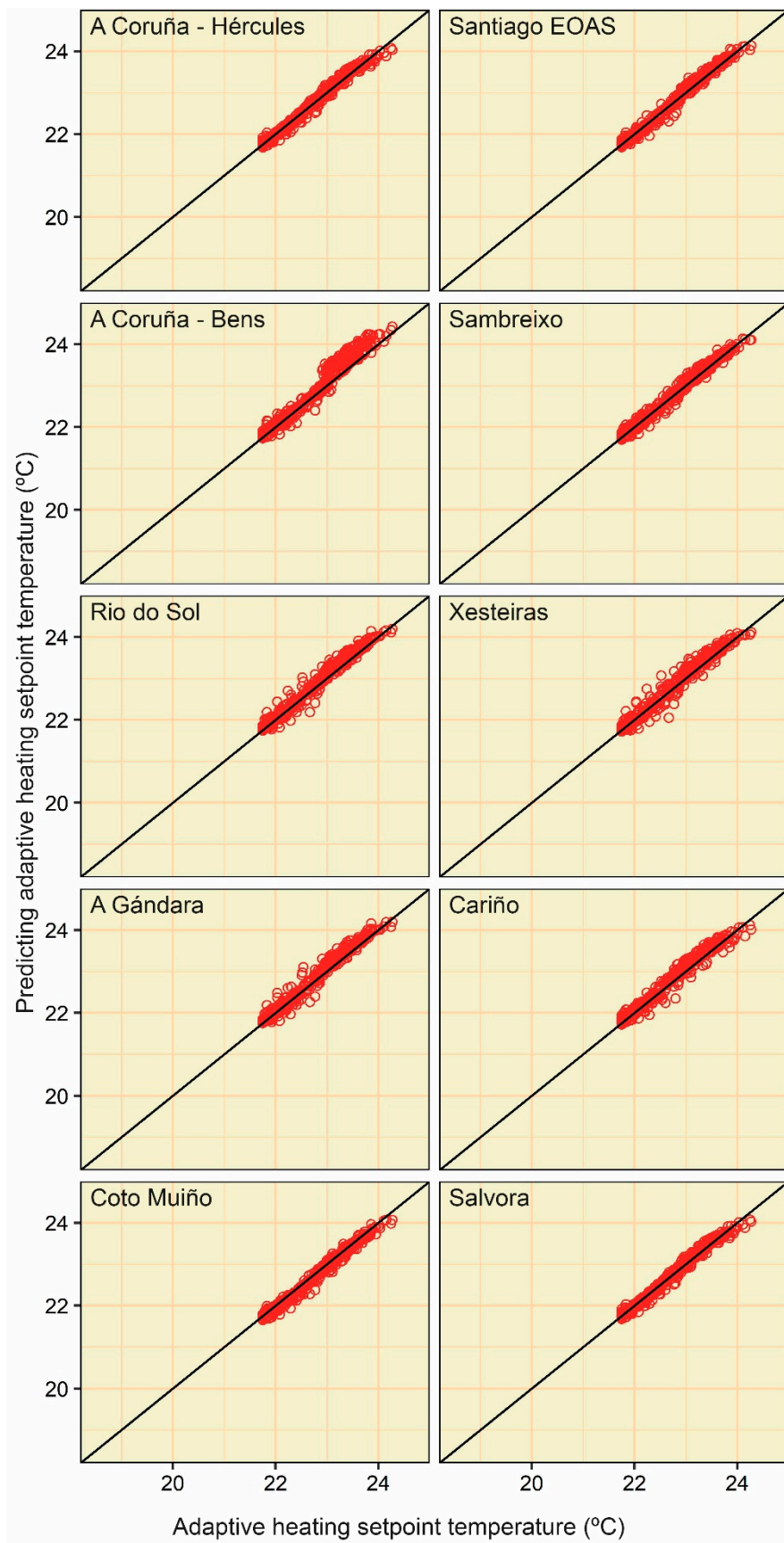


Figure A16. Point clouds between the actual and predicting adaptive heating setpoint temperature values (category I) of the MLP (approach 1).

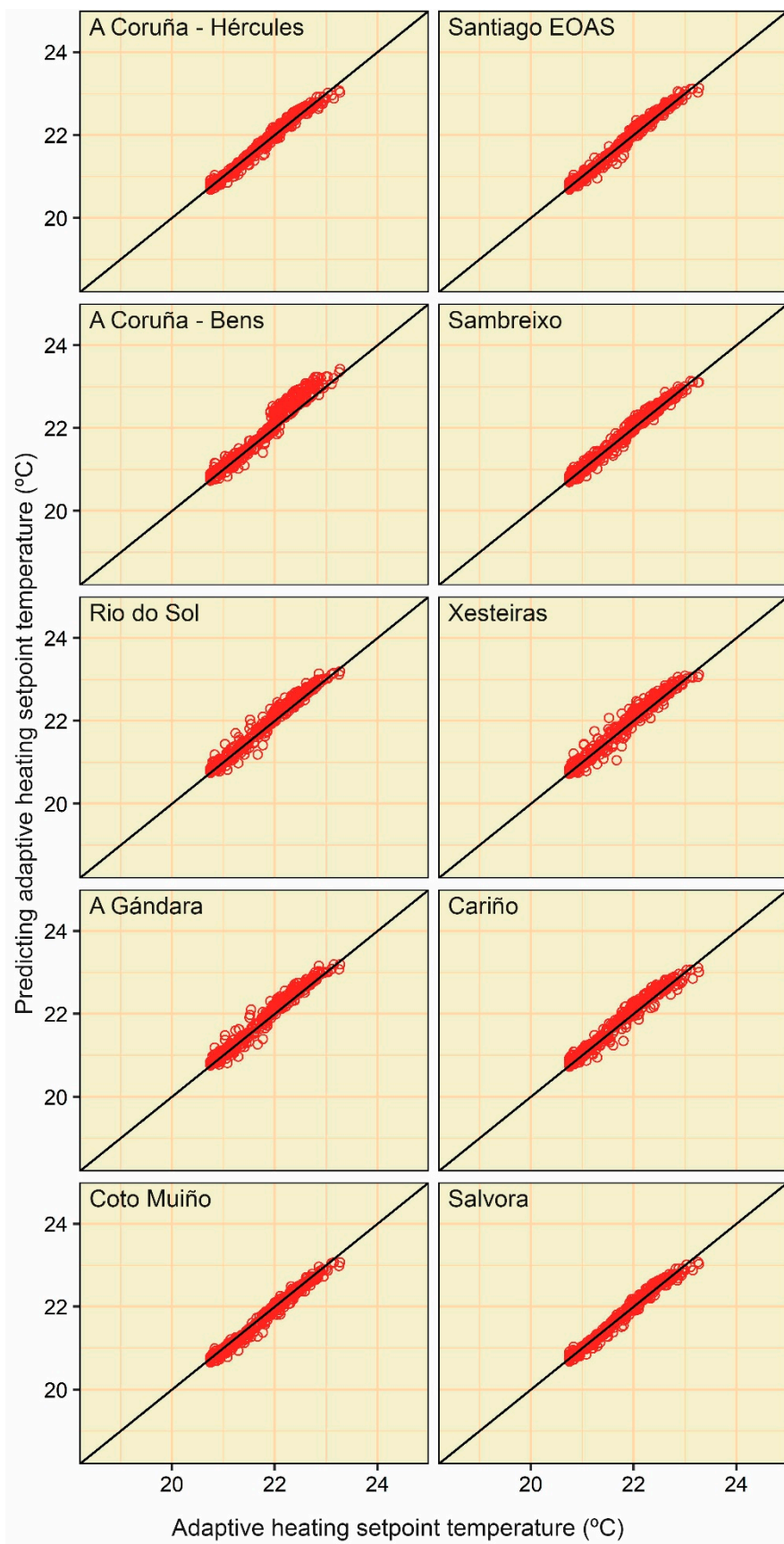


Figure A17. Point clouds between the actual and predicting adaptive heating setpoint temperature values (category II) of the MLP (approach 1).

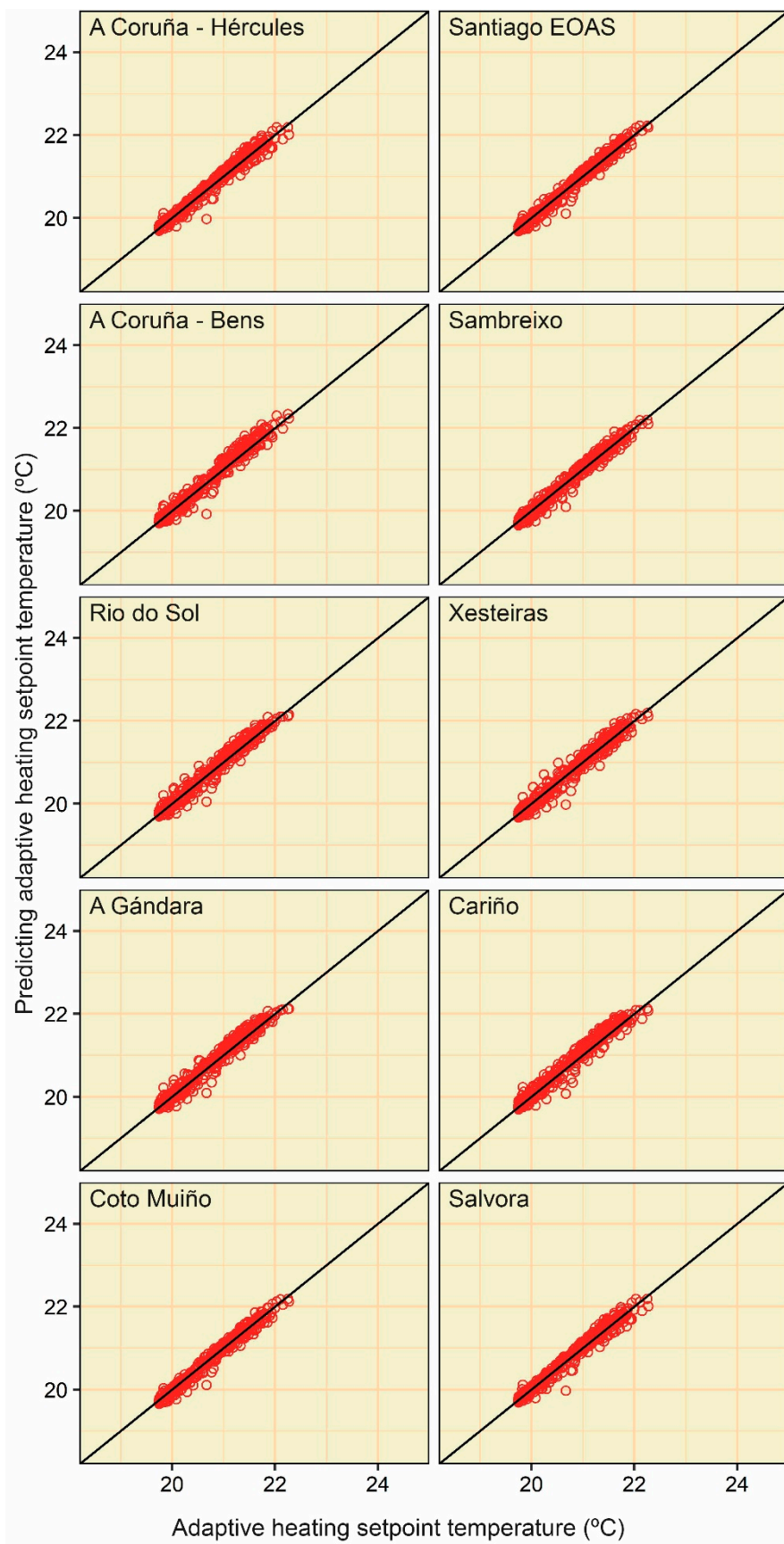


Figure A18. Point clouds between the actual and predicting adaptive heating setpoint temperature values (category III) of the MLP (approach 1).

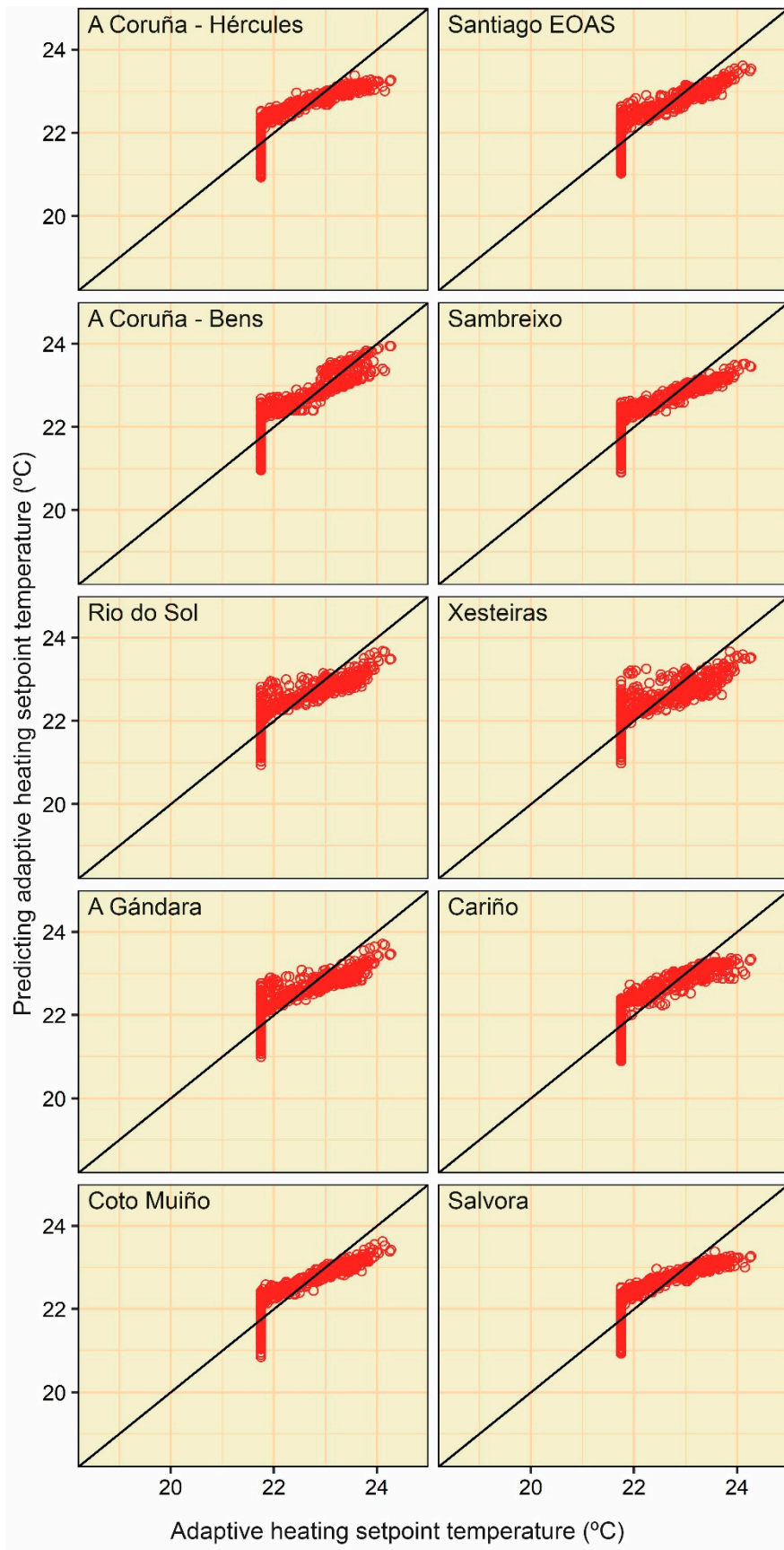


Figure A19. Point clouds between the actual and predicting adaptive heating setpoint temperature values (category I) of the MLR (approach 2).

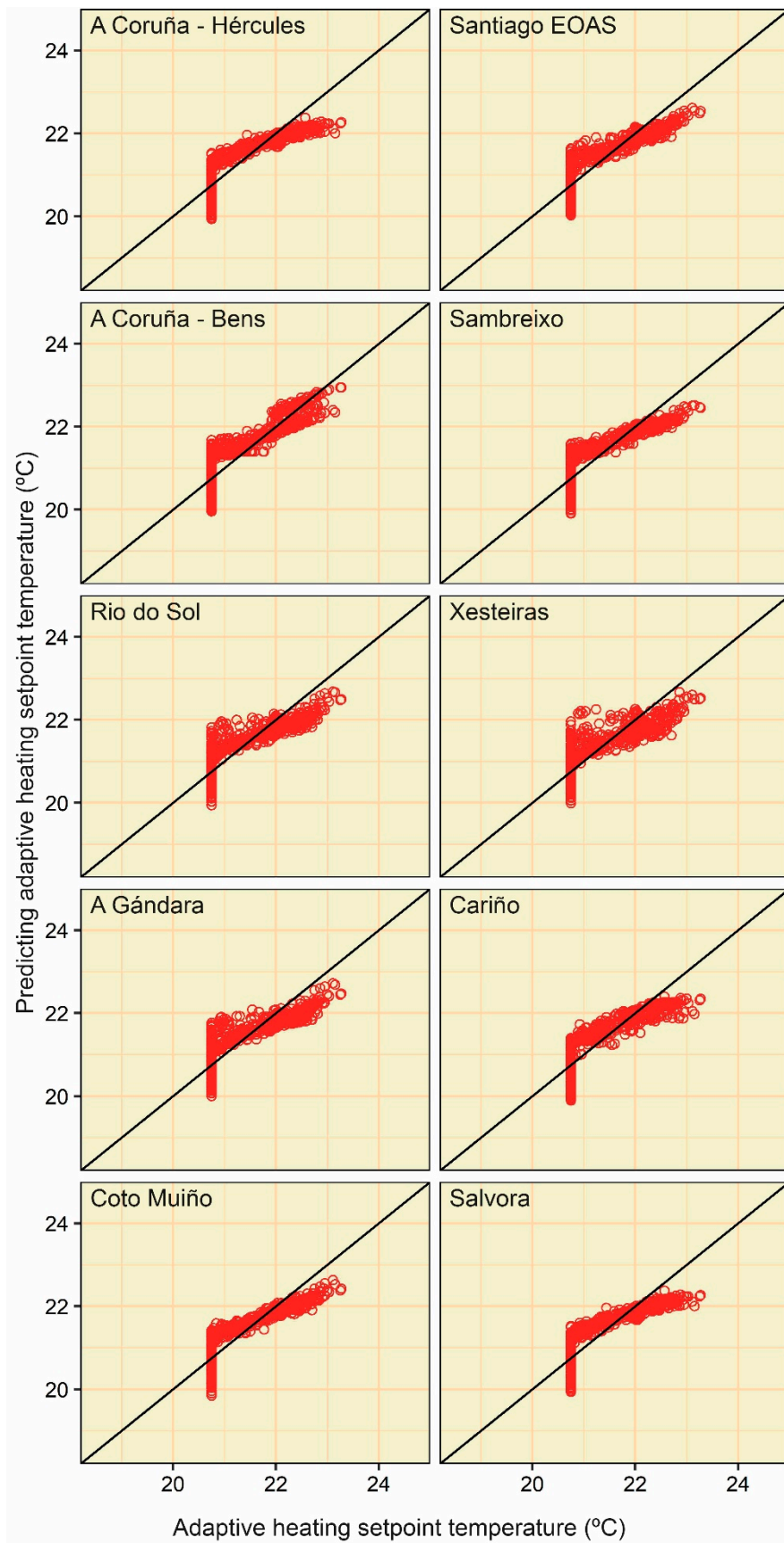


Figure A20. Point clouds between the actual and predicting adaptive heating setpoint temperature values (category II) of the MLR (approach 2).

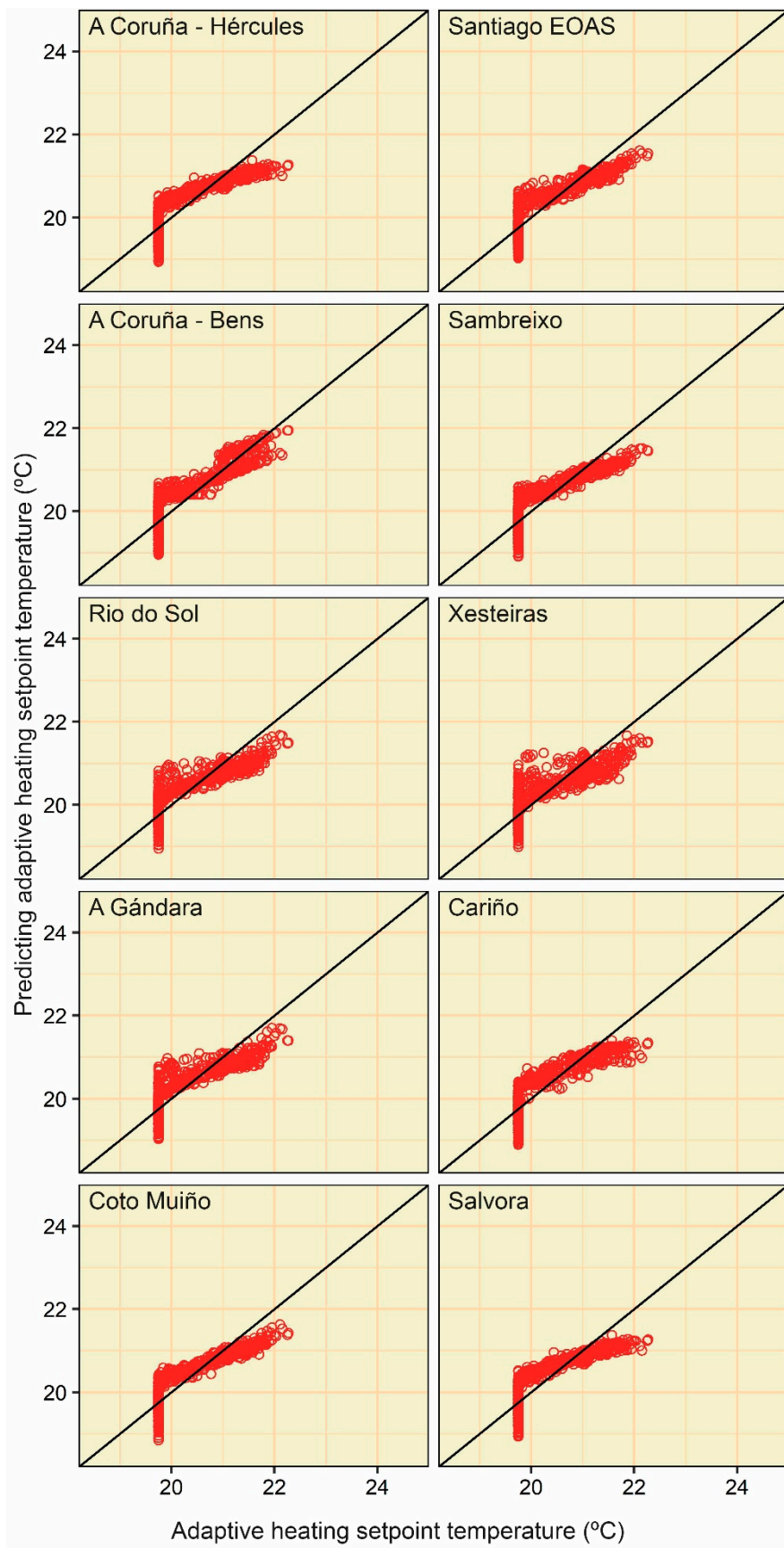


Figure A21. Point clouds between the actual and predicting adaptive heating setpoint temperature values (category III) of the MLR (approach 2).

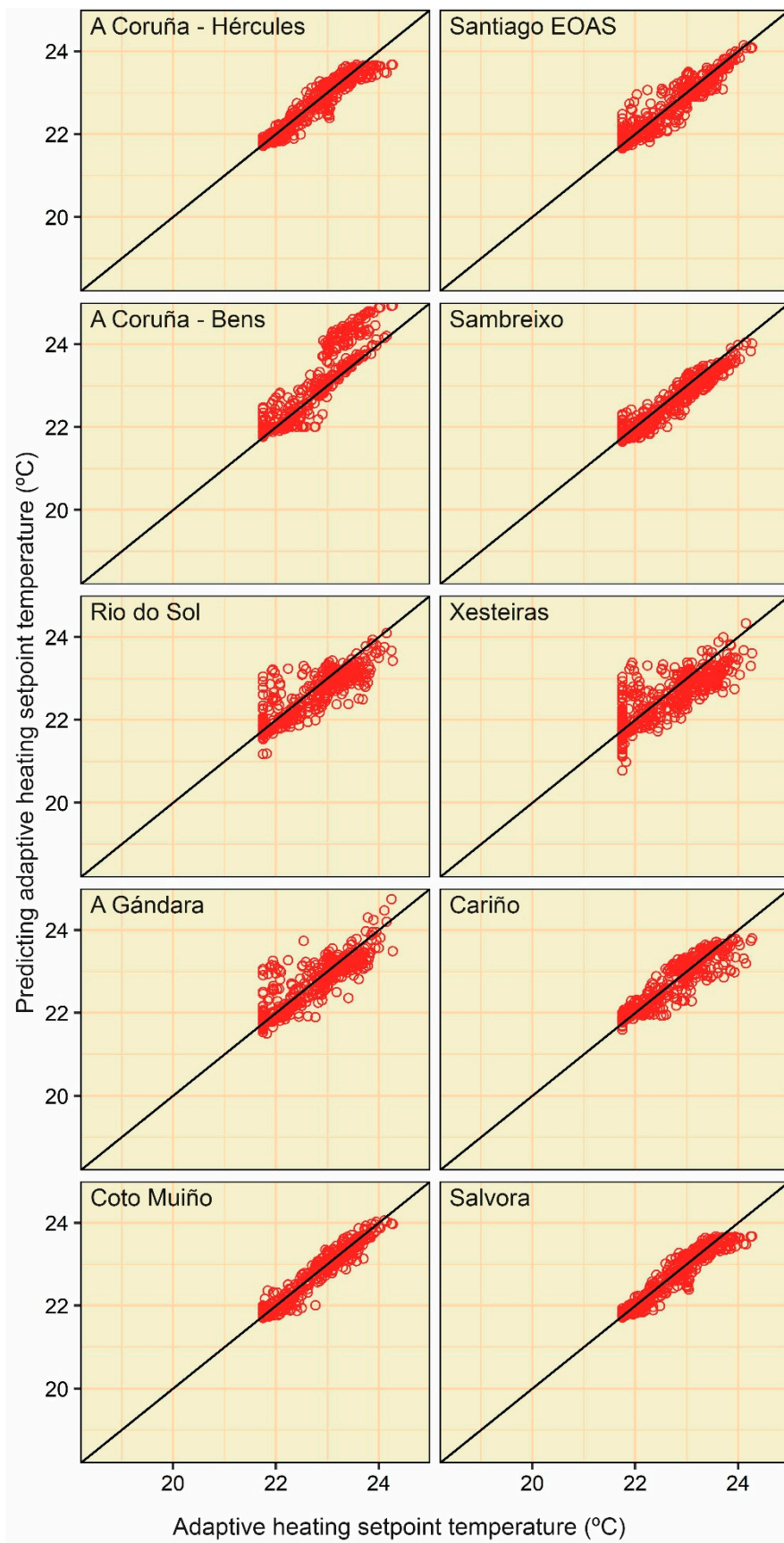


Figure A22. Point clouds between the actual and predicting adaptive heating setpoint temperature values (category I) of the MLP (approach 2).

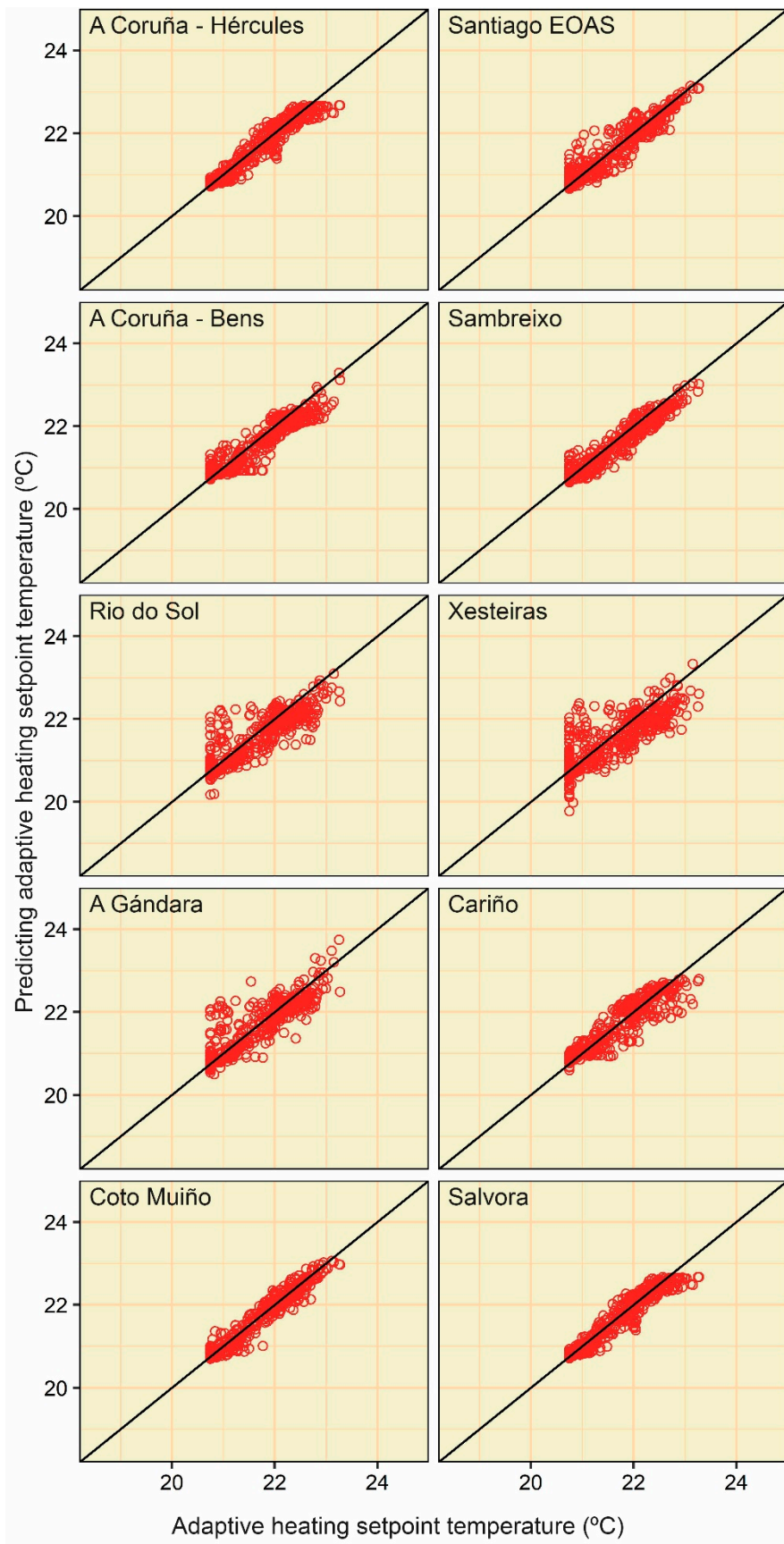


Figure A23. Point clouds between the actual and predicting adaptive heating setpoint temperature values (category II) of the MLP (approach 2).

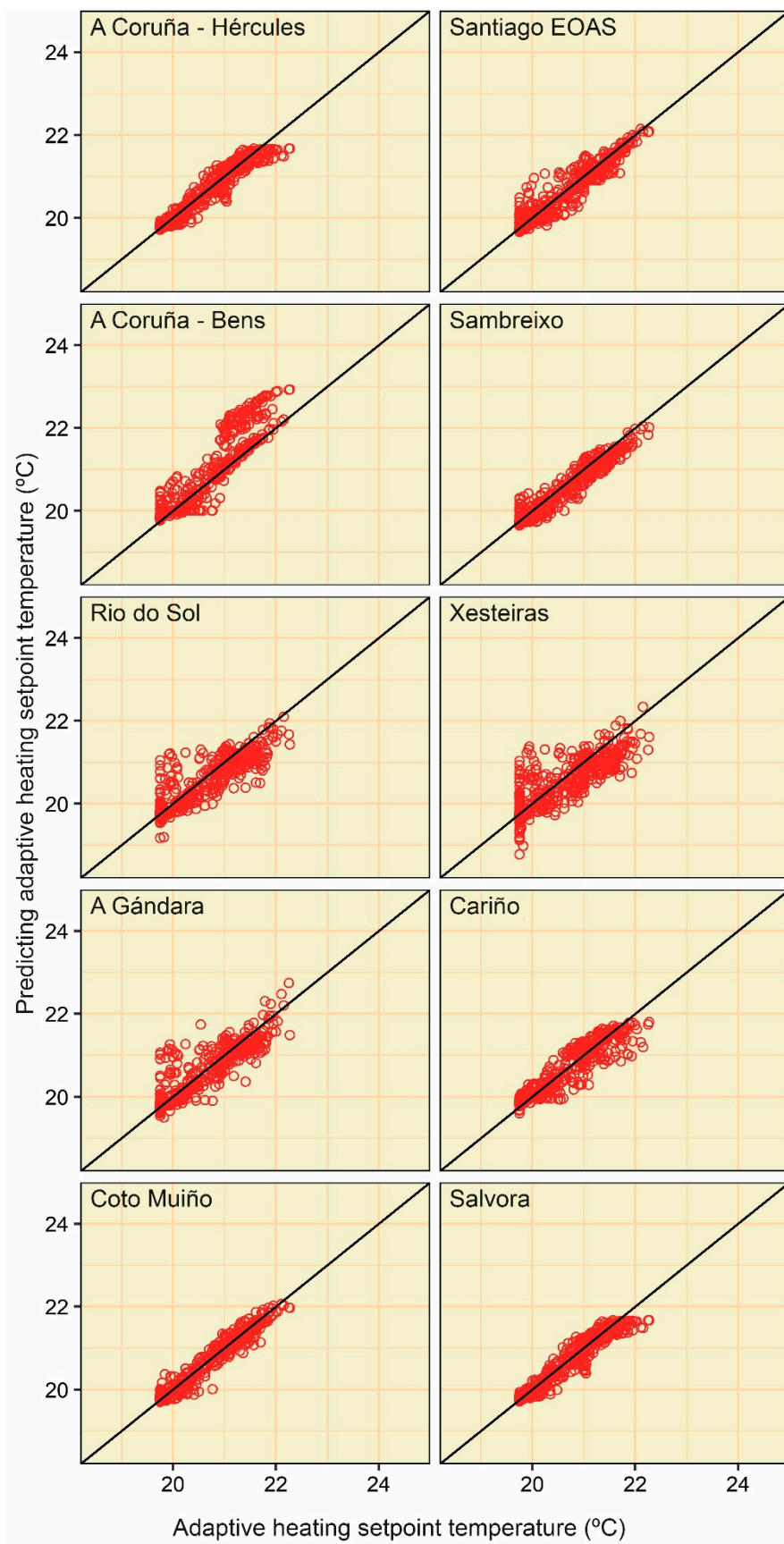


Figure A24. Point clouds between the actual and predicting adaptive heating setpoint temperature values (category III) of the MLP (approach 2).

References

1. World Wildlife Fund. *Living Planet Report 2014: Species and Spaces, People and Places*; WWF International: Gland, Switzerland, 2014; Volume 1, ISBN 9780874216561.
2. The United Nations Environment Programme. *Building Design and Construction: Forging Resource Efficiency and Sustainable*; The United Nations Environment Programme: Nairobi, Kenya, 2012.
3. European Commission Directive 2002/91/EC of the European Parliament and of the council of 16 December 2002 on the energy performance of buildings. *Off. J. Eur. Union* **2002**, 65–71. [[CrossRef](#)]
4. European Union. *Directive 2010/31/EU of the European Parliament and of the Council of 19 May 2010 on the Energy Performance of Buildings*; European Union: Brussels, Belgium, 2010; Volume 153, pp. 13–35.
5. Thomson, H.; Snell, C. Quantifying the prevalence of fuel poverty across the European Union. *Energy Policy* **2013**, 52, 563–572. [[CrossRef](#)]
6. Basu, R.; Samet, J.M. Relation between elevated ambient temperature and mortality: A review of the epidemiologic evidence. *Epidemiol. Rev.* **2002**, 24, 190–202. [[CrossRef](#)]
7. Basu, R. High ambient temperature and mortality: A review of epidemiologic studies from 2001 to 2008. *Environ. Health* **2009**, 8, 40. [[CrossRef](#)]
8. European Commission. *A Roadmap for Moving to a Competitive Low Carbon Economy in 2050*; European Commission: Brussels, Belgium, 2011; pp. 1–15.
9. International Energy Agency. *Energy Efficiency 2017*; International Energy Agency: Paris, France, 2017. [[CrossRef](#)]
10. Spanish Institute of Statistics Population and Housing Census. Available online: https://www.ine.es/censos2011_datos/cen11_datos_resultados.htm# (accessed on 9 November 2018).
11. The Government of Spain. *Royal Decree 314/2006. Approving the Spanish Technical Building Code CTE-DB-HE-1*; The Government of Spain: Madrid, Spain, 2013.
12. Rafsanjani, H.N.; Ahn, C.R.; Alahmad, M. A review of approaches for sensing, understanding, and improving occupancy-related energy-use behaviors in commercial buildings. *Energies* **2015**, 8, 10996–11029. [[CrossRef](#)]
13. Sánchez-García, D.; Rubio-Bellido, C.; Martín del Río, J.; Pérez-Fargallo, A. Towards the quantification of energy demand and consumption through the adaptive comfort approach in mixed mode office buildings considering climate change. *Energy Build.* **2019**. [[CrossRef](#)]
14. Sánchez-García, D.; Rubio-Bellido, C.; Marrero Meléndez, M.; Guevara-García, F.J.; Canivell, J. El control adaptativo en instalaciones existentes y su potencial en el contexto del cambio climático. *Habitat Sustentable* **2017**, 7, 6–17. [[CrossRef](#)]
15. Sánchez-Guevara Sánchez, C.; Mavrogianni, A.; Neila González, F.J. On the minimal thermal habitability conditions in low income dwellings in Spain for a new definition of fuel poverty. *Build. Environ.* **2017**, 114, 344–356. [[CrossRef](#)]
16. Spyropoulos, G.N.; Balaras, C.A. Energy consumption and the potential of energy savings in Hellenic office buildings used as bank branches—A case study. *Energy Build.* **2011**, 43, 770–778. [[CrossRef](#)]
17. Yun, G.Y.; Lee, J.H.; Steemers, K. Extending the applicability of the adaptive comfort model to the control of air-conditioning systems. *Build. Environ.* **2016**, 105, 13–23. [[CrossRef](#)]
18. Hoyt, T.; Arens, E.; Zhang, H. Extending air temperature setpoints: Simulated energy savings and design considerations for new and retrofit buildings. *Build. Environ.* **2014**, 88, 89–96. [[CrossRef](#)]
19. Humphreys, M.A.; Rijal, H.B.; Nicol, J.F. Updating the adaptive relation between climate and comfort indoors; new insights and an extended database. *Build. Environ.* **2013**, 63, 40–55. [[CrossRef](#)]
20. de Dear, R.; Brager, G.S. Thermal comfort in naturally ventilated buildings: Revision to ASHRAE standards 55. *J. Energy Build.* **2002**, 34, 549–561. [[CrossRef](#)]
21. CEN. *EN 15251:2007 Indoor Environmental Input Parameters for Design and Assessment of Energy Performance of Buildings Addressing Indoor Quality, Thermal Environment, Lighting and Acoustics*; European Committee for Standardization: Brussels, Belgium, 2007.
22. Attia, S.; Carlucci, S. Impact of different thermal comfort models on zero energy residential buildings in hot climate. *Energy Build.* **2015**, 102, 117–128. [[CrossRef](#)]
23. Hubbard, K.G.; Lin, X. Realtime data filtering models for air temperature measurements. *Geophys. Res. Lett.* **2002**, 29. [[CrossRef](#)]
24. Albrecht, F. Thermometer zur Messung der wahren Lufttemperatur. *Meteorol. Z.* **1927**, 24, 420–424.

25. Albrecht, F. Über die Einwirkung der Strahlung auf frei aufgestellte elektrische Thermometer. *Veröff. Pruss. Meteorol. Inst.* **1934**, *402*, 76–82.
26. Fuchs, M.; Tanner, C.B. Radiation shields for air temperature thermometers. *J. Appl. Meteorol.* **1965**, *4*, 544–547. [[CrossRef](#)]
27. Anderson, S.P.; Baumgartner, M.F. Radiative heating errors in naturally ventilated air temperature measurements made from buoys. *J. Atmos. Ocean. Technol.* **1998**, *15*, 157–173. [[CrossRef](#)]
28. Huwald, H.; Higgins, C.W.; Boldi, M.O.; Bou-Zeid, E.; Lehning, M.; Parlange, M.B. Albedo effect on radiative errors in air temperature measurements. *Water Resour. Res.* **2009**, *45*, 1–13. [[CrossRef](#)]
29. Arck, M.; Scherer, D. A physically based method for correcting temperature data measured by naturally ventilated sensors over snow. *J. Glaciol.* **2001**, *47*, 665–670. [[CrossRef](#)]
30. Georges, C.; Kaser, G. Ventilated and unventilated air temperature measurements for glacier-climate studies on a tropical high mountain site. *J. Geophys. Res. Atmos.* **2002**, *107*, 1–11. [[CrossRef](#)]
31. Nakamura, R.; Mahrt, L. Air temperature measurement errors in naturally ventilated radiation shields. *J. Atmos. Ocean. Technol.* **2005**, *22*, 1046–1058. [[CrossRef](#)]
32. Hardy, D.R.; Vuille, M.; Braun, G.; Keimig, F.; Bradley, R.S. Annual and Daily Meteorological Cycles at High Altitude on a Tropical Mountain. *Bull. Am. Meteorol. Soc.* **1998**, *79*, 1899–1913. [[CrossRef](#)]
33. Lundquist, J.D.; Huggett, B. Evergreen trees as inexpensive radiation shields for temperature sensors. *Water Resour. Res.* **2010**, *46*, 1–5. [[CrossRef](#)]
34. World Meteorological Organization. *Guide to Meteorological Instruments and Methods of Observation*; World Meteorological Organization: Geneva, Switzerland, 2008; ISBN 9789263100085.
35. Erell, E.; Leal, V.; Maldonado, E. Measurement of air temperature in the presence of a large radiant flux: An assessment of passively ventilated thermometer screens. *Bound.-Layer Meteorol.* **2005**, *114*, 205–231. [[CrossRef](#)]
36. Spanish Institute of Statistics Surface Extension of the Autonomous Communities and Provinces, by Altimetric Zones. Available online: <http://www.ine.es/inebaseweb/pdfDispacher.do?td=154090&L=0> (accessed on 10 January 2019).
37. Spanish Institute of Statistics Population by Autonomous Communities and Cities And Sex. Available online: <https://www.ine.es/jaxiT3/Tabla.htm?t=2853&L=0> (accessed on 10 January 2019).
38. Rubel, F.; Kottek, M. Observed and projected climate shifts 1901–2100 depicted by world maps of the Köppen–Geiger climate classification. *Meteorol. Z.* **2010**, *19*, 135–141. [[CrossRef](#)]
39. Dahlgren, R.A.; Boettinger, J.L.; Huntington, G.L.; Amundson, R.G. Soil development along an elevational transect in the western Sierra Nevada, California. *Geoderma* **1997**, *78*, 207–236. [[CrossRef](#)]
40. Franzmeier, D.P.; Pedersen, E.J.; Longwell, T.J.; Byrne, J.G.; Losche, C.K. Properties of Some Soils in the Cumberland Plateau as Related to Slope Aspect and Position. *Soil Sci. Soc. Am. J.* **1969**, *33*, 755–761. [[CrossRef](#)]
41. Tsui, C.C.; Chen, Z.S.; Hsieh, C.F. Relationships between soil properties and slope position in a lowland rain forest of southern Taiwan. *Geoderma* **2004**, *123*, 131–142. [[CrossRef](#)]
42. Yimer, F.; Ledin, S.; Abdelkadir, A. Soil property variations in relation to topographic aspect and vegetation community in the south-eastern highlands of Ethiopia. *For. Ecol. Manag.* **2006**, *232*, 90–99. [[CrossRef](#)]
43. Eguía Oller, P.; Alonso Rodríguez, J.M.; Saavedra González, Á.; Arce Fariña, E.; Granada Álvarez, E. Improving the calibration of building simulation with interpolated weather datasets. *Renew. Energy* **2018**, *122*, 608–618. [[CrossRef](#)]
44. Ahmad, A.; Maslehuddin, M.; Al-Hadhrami, L.M. In situ measurement of thermal transmittance and thermal resistance of hollow reinforced precast concrete walls. *Energy Build.* **2014**, *84*, 132–141. [[CrossRef](#)]
45. Pino-Mejías, R.; Pérez-Fargallo, A.; Rubio-Bellido, C.; Pulido-Arcas, J.A. Comparison of linear regression and artificial neural networks models to predict heating and cooling energy demand, energy consumption and CO₂ emissions. *Energy* **2017**, *118*, 24–36. [[CrossRef](#)]
46. Pulido-Arcas, J.A.; Pérez-Fargallo, A.; Rubio-Bellido, C. Multivariable regression analysis to assess energy consumption and CO₂ emissions in the early stages of offices design in Chile. *Energy Build.* **2016**, *133*, 738–753. [[CrossRef](#)]
47. Qiang, G.; Zhe, T.; Yan, D.; Neng, Z. An improved office building cooling load prediction model based on multivariable linear regression. *Energy Build.* **2015**, *107*, 445–455. [[CrossRef](#)]

48. Amber, K.P.; Aslam, M.W.; Mahmood, A.; Kousar, A.; Younis, M.Y.; Akbar, B.; Chaudhary, G.Q.; Hussain, S.K. Energy consumption forecasting for university sector buildings. *Energies* **2017**, *10*, 1579. [[CrossRef](#)]
49. Kialashaki, A.; Reisel, J.R. Modeling of the energy demand of the residential sector in the United States using regression models and artificial neural networks. *Appl. Energy* **2013**, *108*, 271–280. [[CrossRef](#)]
50. Asadi, S.; Amiri, S.S.; Mottahedi, M. On the development of multi-linear regression analysis to assess energy consumption in the early stages of building design. *Energy Build.* **2014**, *85*, 246–255. [[CrossRef](#)]
51. Wasserman, P.D. Neural computing: Theory and practice. N. Y. *Van Nostrand Reinhold* **1989**. [[CrossRef](#)]
52. Kandananond, K. Forecasting electricity demand in Thailand with an artificial neural network approach. *Energies* **2011**, *4*, 1246–1257. [[CrossRef](#)]
53. Pino-Mejías, R.; Pérez-Fargallo, A.; Rubio-Bellido, C.; Pulido-Arcas, J.A. Artificial neural networks and linear regression prediction models for social housing allocation: Fuel Poverty Potential Risk Index. *Energy* **2018**, *164*, 627–641. [[CrossRef](#)]
54. Attoue, N.; Shahrour, I.; Younes, R. Smart building: Use of the artificial neural network approach for indoor temperature forecasting. *Energies* **2018**, *11*, 395. [[CrossRef](#)]
55. Zabada, S.; Shahrour, I. Analysis of heating expenses in a large social housing stock using artificial neural networks. *Energies* **2017**, *10*, 2086. [[CrossRef](#)]
56. Yu, W.; Li, B.; Lei, Y.; Liu, M. Analysis of a residential building energy consumption demand model. *Energies* **2011**, *4*, 475–487. [[CrossRef](#)]
57. Deb, C.; Eang, L.S.; Yang, J.; Santamouris, M. Forecasting diurnal cooling energy load for institutional buildings using Artificial Neural Networks. *Energy Build.* **2016**, *121*, 284–297. [[CrossRef](#)]
58. Moon, J.W.; Chin, K.-I.; Kim, S. Optimum application of thermal factors to artificial neural network models for improvement of control performance in double skin-enveloped buildings. *Energies* **2013**, *6*, 4223–4245. [[CrossRef](#)]
59. Akaike, H. A New Look at the Statistical Model Identification. *IEEE Trans. Autom. Control* **1974**. [[CrossRef](#)]
60. Bienvenido-Huertas, D.; Moyano, J.; Rodríguez-Jiménez, C.E.; Marín, D. Applying an artificial neural network to assess thermal transmittance in walls by means of the thermometric method. *Appl. Energy* **2019**, *233–234*, 1–14. [[CrossRef](#)]
61. Fletcher, R. *Practical Methods of Optimization*; John Wiley & Sons: Chichester, UK; New York, NY, USA; Brisbane, Australia; Toronto, ON, Canada, 1980; ISBN 9780471277118.
62. Kohavi, R. A Study of Cross-Validation and Bootstrap for Accuracy Estimation and Model Selection. In Proceedings of the International Joint Conference on Artificial Intelligence, Montreal, QC, Canada, 20–25 August 1995; Volume 5.



© 2019 by the authors. Licensee MDPI, Basel, Switzerland. This article is an open access article distributed under the terms and conditions of the Creative Commons Attribution (CC BY) license (<http://creativecommons.org/licenses/by/4.0/>).